Published in final edited form as:

Arterioscler Thromb Vasc Biol. 2021 September ; 41(9): 2431–2451. doi:10.1161/ATVBAHA.121.316219.

Salt-inducible kinase 3 promotes vascular smooth muscle cell proliferation and arterial restenosis by regulating AKT and PKA-CREB signaling

Yujun Cai[1,2,*], **Xue-Lin Wang**[2], **Jinny Lu**[2], **Xin Lin**[3], **Jonathan Dong**[2], **Raul J Guzman**[1,2,*]

[1]Division of Vascular Surgery and Endovascular Therapy, Department of Surgery, Yale University School of Medicine, New Haven, CT 06510;

[2]Division of Vascular and Endovascular Surgery, Department of Surgery, Beth Israel Deaconess Medical Center, Harvard Medical School, Boston, MA 02215;

[3]Channing Division of Network Medicine, Brigham and Women's Hospital, Harvard Medical School, Boston, MA 02115.

Abstract

Objective-—Arterial restenosis is the pathological narrowing of arteries after endovascular procedures, and it is an adverse event that causes patients to experience recurrent occlusive symptoms. Following angioplasty, vascular smooth muscle cells (SMCs) change their phenotype, migrate, and proliferate, resulting in neointima formation, a hallmark of arterial restenosis. Salt-inducible kinases (SIKs) are a subfamily of the AMP-activated protein kinase family that play a critical role in metabolic diseases including hepatic lipogenesis and glucose metabolism. Their role in vascular pathological remodeling, however, has not been explored. In this study, we aimed to understand the role and regulation of SIK3 in vascular SMC migration, proliferation, and neointima formation.

Approach and Results-—We observed that SIK3 expression was low in contractile aortic SMCs but high in proliferating SMCs. It was also highly induced by growth medium *in vitro* and in neointimal lesions *in vivo*. Inactivation of SIKs significantly attenuated vascular SMC proliferation and up-regulated $p21^{CIP1}$ and $p27^{KIP1}$. SIK inhibition also suppressed SMC migration and modulated actin polymerization. Importantly, we found that inhibition of SIKs reduced neointima formation and vascular inflammation in a femoral artery wire injury model. In mechanistic studies, we demonstrated that inactivation of SIKs mainly suppressed SMC proliferation by down-regulating AKT and PKA-CREB signaling. CRTC3 signaling likely contributed to SIK inactivation-mediated anti-proliferative effects.

[*]**Corresponding authors:** Yujun Cai, PhD, Division of Vascular Surgery and Endovascular Therapy, Department of Surgery, Yale University School of Medicine, New Haven, CT 06510, yujun.cai@yale.edu, Raul J. Guzman, MD, Division of Vascular Surgery and Endovascular Therapy, Department of Surgery, Yale University School of Medicine, New Haven, CT 06510, raul.guzman@yale.edu.

Disclosures

None

Supplemental Materials

Supplemental Table I

Major Resources Table

Conclusions-—These findings suggest that SIK3 may play a critical role in regulating SMC proliferation, migration, and arterial restenosis. This study provides insights into SIK inhibition as a potential therapeutic strategy for treating restenosis in patients with peripheral arterial disease.

Keywords

Salt-inducible kinases; smooth muscle cells; neointimal formation; arterial restenosis

Introduction

Restenosis is the pathological narrowing of blood vessels after endovascular procedures that leads to restricted blood flow. It is an adverse event that causes patients to experience recurrent occlusive symptoms. Every year, more than 1 million endovascular procedures are performed in the US, and restenosis continues to be the leading reason for failure.[1] In the lower extremities, restenosis affects over 60% of patients within 1 year after superficial femoral artery angioplasty and stenting procedures.[2] Under healthy conditions, vascular smooth muscle cells (SMCs) located in the media of arteries are quiescent with expression of a large number of contractile proteins. In response to angioplasty, vascular SMCs modulate their phenotype from a contractile to a synthetic state showing decreased contractile proteins.[3, 4] This leads to migration, proliferation, monocyte/macrophage infiltration, and extracellular matrix deposition, which ultimately results in neointima formation, a hallmark of restenosis.[5–7] Despite extensive efforts to prevent it, restenosis continues to limit our ability to provide durable, minimally invasive treatments for our patients, and its causative mechanisms have not been fully elucidated.

The salt-inducible kinases (SIKs) are a subfamily of the AMP-activated protein kinase (AMPK) family. They contain three isoforms named SIK1, SIK2, and SIK3, which have been demonstrated to play important roles in modulating various cell signaling pathways and biological functions including cell growth.[8–12] Several studies have demonstrated that SIK isoforms play differential roles in the initiation and progression of human diseases. For example, SIK1 has been shown to play critical roles in metastatic tumors. Deletion of SIK1 can facilitate lung metastasis in mice and inactivation of SIK1 can reduce p53 function in anoikis and allow cells to grow in an anchorage-independent manner.[13] SIK2 can attenuate proliferation and survival of breast cancer cells through regulating MAPK and PI3K/Akt pathways.[14] SIK3 has been identified as a novel tumor antigen in ovarian cancer. Overexpression of SIK3 markedly promoted cell proliferation by attenuating $p21^{Waf/Cip1}$ and $p27^{Kip}$ expressions in low-grade ovarian cancer cells.[15] SIK3 has also been shown to act as a key mediator of the tumor-suppressive effects of LKB1, as well as a novel mitotic regulator. Targeting it could enhance antimitotic therapeutic cell death.[16] A recent study has demonstrated that SIK1 is associated with arterial blood pressure and vascular remodeling. Activation of SIK1 reduces high-salt-induced systolic blood pressure through regulation of TGF-β1-mediated vascular SMC phenotypic modulation. However, the function and regulation of SIKs in vascular diseases remain largely unknown.

In this study, we report that SIK3 is the most highly expressed among three SIK isoforms in synthetic SMCs. It is also increased in neointimal lesions during arterial restenosis in a

rodent model, and pharmacological inactivation of SIKs using small molecules is capable of suppressing SMC migration and proliferation, as well as neointima formation. The underlying mechanisms primarily involve modulating both AKT and PKA-CREB signaling pathways.

Material and Methods

The author declare that all supporting data are available within the article (and its Data Supplement).

Animals

All animal care and procedures were conducted in accordance with animal protocols that were approved by the University Animal Care and Use Committee at Beth Israel Deaconess Medical Center and Yale University. C57BL/6J mice were obtained from The Jackson Laboratory and anesthetized with inhaled isoflurane. To study the role of SIKs in arterial restenosis, the neointimal formation was induced by inserting a wire in the femoral artery as described previously.[17, 18] To reduce variability, we used male mice in the femoral artery wire injury model.

Reagents

HG-9–91–01 was purchased from APExBIO (Boston, MA). MRT67307 and MC1568 were from Cayman Chemical (Ann Arbor, MI). Forskolin, Dibutyryl-cAMP (db-cAMP), H89 and PKI (14–22) Amide were obtained from Enzo Life Sciences (Farmingdale, NY). 666–15 was purchased from MCE MedChem Express (Monmouth Junction, NJ), LY294002 was from Cell Signaling Technology. Other reagents were purchased from Millipore Sigma (St. Louis, MO).

Femoral artery wire injury

The femoral artery wire injury procedure was conducted as described previously.[17, 18] Briefly, 10 week-old male C57BL/6J mice were anesthetized with inhaled isoflurane, and the left femoral artery was isolated and temporarily looped proximally and distally with 6–0 silk suture. A small branch artery between the rectus femoris and vastus medialis muscles was dissected and ligated with 6–0 silk suture. A small transverse arteriotomy was performed on this artery. A 0.38 mm in diameter straight spring wire (COOK, Bloomington, IN, catalog No. CSF-15–15) was carefully inserted into the femoral artery and kept for 1 min to denude the vessel. A 50 μl of 20% pluronic F-127 gel containing 10 μM of SIK inhibitor HG-9–91–01 or vehicle was immediately applied around the injured vessel. 4 weeks later, the animals were perfused with saline and 10% phosphate-buffered formalin (NBF). The femoral arteries were isolated and fixed, and the paraffin sections were prepared.

Morphometric analysis

After animals were perfused with saline and 10% NBF, the femoral arteries were dissected, fixed, and embedded in paraffin. 6–10 cross-sections located at 200 μm intervals from the bifurcation for each vessel were cut and stained with Hematoxylin and eosin (H&E) and Verhoeff-Van Gieson (VVG). The areas of lumen, intima, and media were measured by

ImageJ software. The intimal area was calculated as the internal elastic lamina area minus luminal area, and the medial area was the external elastic lamina area minus the internal elastic lamina area.

Rat aortic SMC isolation and culture

Rat aortic SMCs were prepared using enzymatic digestion of thoracic aortas from 10 week-old male or female Sprague-Dawley (SD) rats as described previously.[19] Rat aortic SMCs were cultured in Dulbecco's Modified Eagle's Medium (DMEM) containing 10% FBS and 1% pen/strep in a humidified incubator (37°, 5% CO_2). Passage 6 to 8 was used for the experiments.

Preparation of rat synthetic and contractile SMCs

Synthetic rat aortic SMCs were prepared using an explant method.[17] Briefly, rat aorta was dissected from 10 week-old male and female SD rat and digested with type 2 collagenase (Worthington Biochemical, CLS 2) for 10 min at 37°C. After the adventitia was peeled off and the endothelial layer was scraped using a cotton swab, the media was cut in half. Half media was cut into small pieces and then cultured in 10% FBS DMEM growth medium, which refers to synthetic rat aortic SMCs. Synthetic SMCs at passage 4 were used to isolate RNA. Another half media (mainly contractile SMCs) was directly used to isolate RNA.

Cell proliferation assessment

A sulforhodamine-B (SRB) colorimetric assay was used to measure SMC proliferation as described previously.[20, 21] Briefly, rat aortic SMCs were plated in 96-well plates overnight in DMEM with 10% FBS. After serum starvation, cells were stimulated with 5% FBS or 50 ng/ml PDGF-BB for 2 days. At the end of the experiment, cells were fixed with 10% trichloroacetic acid (TCA), stained with 4 mg/ml SRB, and dissolved with 10 mM Tris base. Optical density at 515 nm was measured using a VERSAmax microplate reader (Molecular Devices).

Scratch wound-healing assay

SMC migration was assessed using a wound-healing assay as described previously.[21, 22] Confluent SMCs in 35 mm dishes were starved and then scratched with a 100 μl pipette tip, followed by stimulation of 5% FBS for 6 h. The cells were fixed with 4% paraformaldehyde (PFA), and the images were captured using by EVOS XL Core Cell Imaging System (ThermoFisher Scientific). Quantification was made by ImageJ software.

Modified Boyden chamber assay

The migration of SMCs was also measured using a modified Boyden chamber assay as described previously.[21] 100 μl rat aortic SMCs (5×10^5 cells/ml) in DMEM with 0.5% FBS were seeded in the insert chamber (6.5 mm diameter, 8.0 μm pore size, Corning Inc) and 600 μl DMEM with 5% FBS was added into the bottom well in a 24-well plate, and the plate was incubated at 37°C and 5% CO_2 for 6 h. Next, the cells on the upper side of the filter membrane were scraped off with cotton tips, and the filter was fixed in 4% PFA

and stained with hematoxylin. The images were captured by EVOS XL Core Cell Imaging System (ThermoFisher Scientific).

Aortic media explant migration assay

The migration of SMCs was also assessed by a 3-D aortic media explant migration assay as described previously.[17, 23] Briefly, after the thoracic aortas were collected from mice, the adventitia was stripped by collagenase type II digestion and the endothelium layer was removed by cotton swabs. The media was cut into 1 ×1 mm explants and then embedded in 2 mg/ml type I collagen gel in 24-well plates and cultured in DMEM containing 10% FBS, 10 ng/ml PDGF-BB, and 10 ng/ml FGF-2 for 10 days. The migration was quantified by measuring the distance migrated by the leading front of SMCs from the explanted tissue.

Cell cycle analysis

The distribution of SMCs in the cell cycle was examined by flow cytometry analysis as described previously.[21, 24] Briefly, the cultured SMCs were serum-starved for 2 days, then stimulated with 5% FBS with or without SIK inhibitor HG-9–91–01 for 24 h. At the end of the experiment, cells were fixed with 70% ethanol/PBS at 4°C, treated with 10 μg/ml RNase A solution at 37°C for 15 min, and then stained with 10 μg/ml propidium iodide at room temperature in the dark for 0.5 h. At least 1×10^4 cells were analyzed using a BD FACSCalibur cytometer (BD Biosciences), and the cell population in each cell cycle phase was calculated using BD CellQuest Pro software.

Cytoskeletal F-actin assessment

F-actin cytoskeleton was determined using Phalloidin CruzFluor™ 594 Conjugate (Santa Cruz Technology, sc-363795) staining. In brief, SMCs were seeded in on 4-well cell culture slides (MatTek) and serum-starved for 2 days, and then stimulated with 5% FBS with or without SIK inhibitor HG-9–91–01 for 16 h. Cells were fixed with 4% PFA, permeabilized in 0.2% Triton X-100, and stained with Phalloidin CruzFluor™ 594 Conjugate. The nuclei were stained with DAPI. Images of F-actin cytoskeleton were captured with a Zeiss AxioImager M1 microscope and qualified by ImageJ software.

siRNA transfection

Rat SIK3 siRNA (CAGUCAAUAUCCAGGCGGA) was designed and synthesized by Millipore Sigma. Rat CREB siRNA was purchased from Santa Cruz Biotechnology (sc-72030). Rat HDAC4 siRNA was obtained from Cell signaling technology, Inc (#759). Rat aortic SMCs were transfected with SIK3 siRNA or CREB siRNA using Lipofectamine RNAi/MAX reagent (ThermoFisher Scientific, 13778–075) according to manufacturer's instructions.

Quantitative PCR

Total RNA was isolated from rat aortic SMCs using RNeasy Mini Kit (Qiagen, Hilden, Germany). cDNA was synthesized using iScript cDNA Synthesis Kit (Bio-Rad, 170–8890). Quantitative PCR (qPCR) amplifications were performed using PowerUp™ SYBR® Green Master Mix (ThermoFisher Scientific, A25742) in Applied Biosystems 7500 Fast Real-Time

PCR System. The relative mRNA levels were obtained using the comparative Ct method and normalized with internal control glyceraldehyde-3-phosphate dehydrogenase (GAPDH). The primers used for qPCR were listed in Supplemental Table I.

Western blot

SMCs were lysed in RIPA buffer with protease inhibitor Cocktail (Millipore Sigma, P8340). The concentrations of total proteins were measured using the Pierce BCA Protein Assay Kit (ThermoFisher Scientific, 23225). 10 μg of cell lysates was loaded on SDS-PAGE and electro-transferred into PVDF membrane at 4°C overnight. The membranes were then incubated with horseradish peroxidase-coupled secondary antibodies at room temperature for 2 h. The signals were visualized using Amersham ECL Western Blotting Detection Reagent (GE Healthcare Life Science, RPN2106). The primary antibodies against AKT (Cell signaling technology, #9272), p-AKT (Cell signaling technology, #9271), Erk (Cell signaling technology, #9102), p-Erk (Cell signaling technology, #9101), p-Ser^{157} VASP (Enzo Life Sciences, ALX-804–403-C200), CREB (Cell signaling technology, #9197), p-CREB (Cell signaling technology, #9198), SIK3 (LSBio, LS-B9603), HDAC4 (Santa Cruz Biotechnology, sc-46672), GAPDH (Millipore Sigma, MAB374) and α-Tubulin (Millipore Sigma, T5168) were used in this study.

Immunofluorescent staining

SMCs were seeded on 4-well cell culture slides (MatTek), fixed in 4% PFA, permeabilized in 0.1% Triton x-100/PBS, and blocked with Dako serum-free blocking solution (Dako, X090930). The immunofluorescent staining was conducted using the primary antibody, followed by incubation of secondary antibody Alexa Fluor 546 or 488 (ThermoFisher Scientific). The primary antibodies against BrdU (Bio-Rad, MCA2483T) and CRTC3 (Abcam, ab91654) were used. Nuclei were stained with DAPI. The staining was visualized with Zeiss AxioImager M1 microscope.

Immunohistochemistry

Femoral arteries were dissected and embedded in paraffin, and cross-sections were cut at 200 μm intervals. The sections were deparaffinized and treated with citrate buffer for antigen retrieval, followed by incubation in 3% H_2O_2. The sections were then blocked with Dako serum-free blocking solution (Dako, X090930) and incubated with primary antibody at 4°C overnight. Next, the sections were incubated with biotinylated secondary antibodies for 30 min at room temperature. VECTASTAIN ABC HRP kit (Vector Laboratories, PK-4000) and DAB peroxidase substrate kit (Vector Laboratories, SK-4100) were used for detection. Hematoxylin was used for nuclear counterstaining. The primary antibodies used in this study are anti-SIK3 (LSBio, LS-B9603), anti-SM-α-actin (Dako, M0851), anti-PCNA (Santa Cruz, sc-56), and anti-Mac2 (Cedarlane, CL8942AP). The matched IgG was used for negative control. Slides were visualized, and images were captured by Zeiss AxioImager M1 microscope.

Statistical analysis

Data are represented as mean ± SD or mean ± SE. Statistical analyses were performed using GraphPad Prism 6.0 software. Data were analyzed by t-test, one-way ANOVA or two-way ANOVA with multiple comparisons. ANOVA analysis was corrected with post hoc test. The data have been confirmed for normality and equal variance as a justification for using parametric analysis. $P<0.05$ was considered statistically significant.

Results

SIK3 is highly expressed in growing SMCs *in vitro* as well as neointimal lesions *in vivo*

SIKs contain three isoforms, SIK1, 2, and 3. To determine whether SIKs are differentially expressed in contractile and growing SMCs, we performed real-time PCR to compare the three SIK mRNA levels in contractile SMCs (normal aortic medial SMCs) and growing SMCs (cultured aortic SMCs). As shown in Figure 1A, SIK3 was highly expressed in growing SMCs compared with medial SMCs among the three SIKs (≥18 folds). To further investigate if SIK3 is specifically induced during SMC growth, rat aortic SMCs were starved and stimulated with FBS. As expected, SIK3 was exclusively induced by FBS (Figure 1B). These data suggest that SIK3 could be important during SMC proliferation *in vitro*. Next, we used a mouse femoral artery wire injury model that is commonly used for mimicking arterial restenosis to determine whether SIK3 expression was altered in response to injury.[17, 18, 25] As shown in Figure 1C, VVG staining for elastin fibers showed that neointimal formation in the left femoral artery was increased following injury compared with uninjured vessels. Immunohistochemistry (IHC) staining for the SMC marker SM-α-actin showed that SMCs accumulated in the neointima although the intensity of SM-α-actin decreased, likely due to phenotypic change. PCNA-positive staining further confirmed a large proportion of proliferating SMCs in the neointimal lesion. Concomitant with these changes, SIK3 was increased in neointimal lesions and highly expressed in nuclei in response to injury compared with uninjured vessels. To further confirm the finding that SIK3 was induced following wire injury, we performed a real-time PCR for SIK3, SMC contractile marker SM-MHC (MYH11), as well as proliferative marker PCNA in both uninjured and injured femoral arteries. Consistently, in response to injury, SM-MHC expression decreased (Figure 1F), whereas the expression levels of SIK3 and PCNA were significantly increased (Figure 1D–E). These findings suggest that SIK3 may regulate SMC proliferation and arterial restenosis.

Knockdown and inhibition of SIK3 suppress SMC proliferation *in vitro*

To explore whether SIK3 plays a role in vascular SMC proliferation, the specific SIK3 siRNA was used. Cell proliferation was assessed using a sulforhodamine B (SRB) proliferation assay.[17, 21] As shown in Figure 2A–D, SIK3 siRNA specifically decreased SIK3 levels without affecting expression of SIK1 and SIK2 in SMCs. Next, FBS and the growth factor PDGF-BB markedly stimulated proliferation in scrambled siRNA-treated SMCs, however, these effects were significantly suppressed in SIK3 siRNA-treated cells (Figure 2E–F). To test whether inactivation of SIK3 plays a similar role in SMC proliferation, we utilized two SIK inhibitors HG-9–91–01 and MRT67307. As expected, both SIK inhibitors dose-dependently antagonized FBS and PDGF-BB induced SMC

growth (Figure 2G–J). Furthermore, using a BrdU immunofluorescence staining for cell proliferation, we observed that HG-9–91–01 significantly attenuated FBS-induced BrdU incorporation in SMCs (Figure 2K–L). These data suggest that SIK3 could play a key role in regulating SMC proliferation.

SIK inhibition up-regulates $p21^{CIP1}$ and $p27^{KIP1}$ and suppresses SMC proliferation

We next utilized HG-9–91–01 to identify the mechanisms by which SIK3 regulates SMC proliferation. We first performed cell cycle analysis in SMCs. As shown in Figure 3A, the representative flow cytometry data showed that approximately 94% of cells were in the G0/G1 phase when SMCs were serum-free starved. In response to FBS stimulation, the percentage of cells in the G0/G1 phase was markedly decreased (approximately 66%), whereas the cells in S and G2/M phases were increased. However, after treatment with 1 μM of HG-9–91–01, approximately 94% of SMCs accumulated in the G0/G1 phase, which was similar to that in serum-free starvation conditions. Quantitative data showed that HG-9–91–01 dose-dependently blocked FBS-induced cell cycle progression (Figure 3B). It is well known that cyclins control cell cycle progression by activating cyclin-dependent kinase (CKD) enzymes, and $p21^{CIP1}$/$p27^{KIP1}$ can bind to cyclin/CKD complexes to induce cell cycle arrest. Therefore, we examined the expression of cyclins, p21CIP1, p27KIP1, as well as cell proliferation marker PCNA using real-time PCR. As shown in Figure 3C, as expected, SIK inhibition by HG-9–91–01 dose-dependently decreased FBS-induced PCNA expression in SMCs. Accordingly, HG-9–91–01 suppressed FBS-induced up-regulation of Cyclin D, E1 and B1 (Figure 3D–F) and down-regulation of $p21^{CIP1}$ and $p27^{KIP1}$ (Figure 3G–H). These data suggest that SIK inhibition suppresses SMC proliferation likely through up-regulation of $p21^{CIP1}$ and $p27^{KIP1}$.

SIK inactivation attenuates SMC migration and modulates actin polymerization

It is well known that SMC migration is essential for neointima formation of arterial restenosis. Therefore, we assessed the effect of SIK inhibitor HG-9–91–01 on SMC migration. As shown in Figure 4A–C, using a scratch wound-healing assay, we found that FBS stimulation largely gave rise to SMC migration in the scratched area showing decreased scratch gap and increased migration cells. By contrast, HG-9–91–01 treatment dose-dependently attenuated FBS-induced migratory effects. Consistently, using a modified Boyden chamber assay, we also observed that HG-9–91–01 inhibited FBS-induced SMC migration (Figure 4D–E). To be better mimic *in vivo* cell behaviors, we used a 3D *ex vivo* aortic media explant migration assay to evaluate the effects of HG-9–91–01 on SMC migration. As shown in Figure 4F–G, after 10 days of culture, SMCs were grown out of the aortic medial explants in a 3D type I collagen gel system. However, HG-9–91–01 treatment dose-dependently reduced growth factors-induced outgrowth of SMCs. It has been demonstrated that actin polymerization is critical for SMC migration.[26, 27] To examine the effect of SIK inactivation on FBS-induced actin polymerization, we conducted the F-actin cytoskeleton immunostaining using Phalloidin CruzFluor™ 594 Conjugate. As shown in Figure 4H–I, FBS stimulation induced actin polymerization shown by increased F-actin filaments, however, these effects were significantly reduced by the treatment of HG-9–91–01 in a dose-dependent manner. To investigate the role of SIK3 in SMC actin polymerization, we utilized specific SIK3 siRNA. As shown in Figure 4J–K, knockdown of SIK3 inhibited

FBS-induced F-actin expression. These data suggest that SIK3 inactivation suppresses SMC migration likely through modulating actin polymerization.

SIK inhibition reduces neointimal formation following arterial injury

To determine whether SIK inhibition is capable of reducing arterial restenosis *in vivo*, we used the femoral artery wire injury procedure.[18, 25] A total of 10 μM of HG-9–91–01 in 20% pluronic F-127 gel was applied around the femoral artery. As shown in Figure 5A, VVG staining showed that there was no neointima formation in the uninjured arteries. After injury, increased neointimal areas were noted in vehicle-treated mice, however, this effect was significantly reduced in HG-9–91–01 treated mice. The quantitative morphometric analysis indicated that wire injury resulted in a marked increase of neointimal area compared with uninjured vessel (Figure 5B–D). However, HG-9–91–01 application significantly blocked these changes. Because SMC proliferation primarily contributes to neointima formation following injury, we performed IHC staining for SMC marker SM-a-actin and proliferation marker PCNA in the arteries from injured and uninjured animals. As expected, SM-a-actin-positive areas were largely increased in injured arteries compared with uninjured vessels. Accordingly, the expression of PCNA expression was increased in neointimal areas. However, HG-9–91–01 application significantly reduced SMC-positive areas and PCNA-positive cells (Figure 5E–G).

It has been demonstrated that vascular inflammation plays a critical role in the pathogenesis of vascular remodeling. To examine whether SIK inhibition could block vascular inflammation following injury, we performed IHC staining for the inflammatory markers Mac2. As shown in Figure 5E and H, Mac2 was increased in injured arteries compared with uninjured vessels. By contrast, these effects were significantly blunted by HG-9–91–01 application. These data suggest that SIK activation plays a critical role in pathological arterial remodeling, and that SIK inhibition could be a potential therapy to reduce neointima formation.

SIK inactivation suppresses SMC proliferation through inhibition of AKT signaling

It has been demonstrated that growth factor-mediated activation of AKT and ERK1/2 play critical roles in SMC proliferation and neointima formation.[21, 28] To identify the signaling pathways through which SIK3 regulates SMC proliferation, we first examined the effects of SIK inhibition on activation of AKT and ERK. As shown in Figure 6A–C, short-term (0.5 h) and long term (24 h) FBS stimulation dramatically increased phosphorylation of AKT and ERK1/2 even though the levels of phosphorylation were lower at 24 h than at 0.5 h. By contrast, SIK inhibitor HG-9–91–01 dose-dependently attenuated FBS-induced phosphorylation of AKT, however, it had no effect on FBS-induced ERK phosphorylation. HG-9–91–01 also time-dependently inhibited FBS-induced AKT phosphorylation in SMCs (Figure 6D–E). These data suggest that SIK inhibition could specifically regulate AKT signaling pathway. Furthermore, we utilized SIK3 siRNA to investigate whether knockdown of SIK3 is able to affect AKT phosphorylation. As shown in Figure 6F–G, SIK3 siRNA significantly decreased FBS-induced p-AKT compared with Scrambled siRNA. To determine whether HG-9–91–01 mediated the inhibitory effects on SMC proliferation by inhibiting AKT signaling, SMCs were pre-treated with PI3K/AKT inhibitor LY294002

and then treated with HG-9–91–01. As shown in Figure 6H, both LY294002 and HG-9–91–01 significantly suppressed SMC proliferation as expected, however, HG-9–91–01 did not further decrease SMC proliferation in LY294002-treated cells. Moreover, we used a constitutively activated AKT (Myr-AKT) construct. As shown in Figure 6I–J, transfection with Myr-AKT increased expression of both p-AKT and total AKT in SMCs, suggesting activation of AKT signaling. Accordingly, we found that Myr-AKT significantly reduced the inhibitory effect of SIK inhibitor on SMC proliferation. These data suggest that SIK3 inhibition may suppress SMC proliferation through down-regulation of AKT signaling.

SIK inactivation suppresses SMC proliferation through down-regulation of PKA-CREB signaling

It has been demonstrated that PKA-mediated CREB signaling plays an important role in growth factor-induced cell proliferation.[29] To investigate whether SIK inactivation can regulate PKA/CREB signaling, p-Ser157-VASP, a PKA substrate, was examined in SMCs using western blotting. As shown in Figure 7A–B, in response to FBS stimulation, the levels of p-Ser^{157}-VASP were dramatically increased at 15 min and then gradually decreased to serum-free levels at 6 h, however, this effect was significantly reduced by treatment with HG-9–91–01. A similar pattern was observed in FBS-stimulated CREB phosphorylation. (Figure 7A and C). Next, we used SIK3 siRNA to determine whether SIK3 could regulate CREB phosphorylation. As shown in Figure 7D–E, knockdown of SIK3 decreased FBS-induced phosphorylated CREB levels. To identify whether HG-9–91–01 inhibits SMC proliferation through PKA/CREB signaling, we used the PKA inhibitor H89 and the CREB inhibitor 666–15. We first tested if inhibition of PKA or CREB could suppress SMC proliferation. As shown in Figure 7F–G, the treatment of H89 or 666–15 dose-dependently inhibited FBS-induced SMC growth suggesting the importance of PKA/CREB in SMC proliferation. To investigate whether CREB signaling is involved in SIK-mediated proliferation, SMCs were treated with 666–15 combined with HG-9–91–01. As shown in Figure 7H, addition of HG-9–91–01 to 666–15-treated cells did not further decrease SMC proliferation. These data suggest that reducing SIK activity may decrease SMC proliferation by down-regulating PKA/CREB signaling. To further determine the role of CREB in SIK-regulated SMC proliferation, SMCs were transfected with specific CREB siRNA. As shown in Figure 7I, CREB siRNA decreased the levels of CREB and p-CREB in FBS-stimulated SMCs. Interestingly, we did not observe that CREB siRNA suppressed SMC proliferation as CREB inhibitor 666–15 did. Conversely, we observed that CREB knockdown increased FBS-induced SMC growth (Figure 7J).

SIK inactivation suppresses cAMP-triggered CREB signaling

It has been shown that cAMP-mediated PKA-CREB signaling could play an inhibitory role in cell proliferation.[17, 30, 31] To determine the role of SIKs in cAMP-PKA-CREB signaling mediated inhibition of SMC growth, we utilized forskolin, an adenylyl cyclase activator, and db-cAMP, a cell-permeable cAMP analog to increase intracellular cAMP levels. As shown in Figure 8A–B, both forskolin and db-cAMP inhibited FBS-induced SMC proliferation, suggesting that activation of cAMP/PKA/CREB signaling is capable of inhibiting SMC proliferation. To study the effects of SIK inhibition on cAMP/PKA/CREB signaling, SMCs were treated with forskolin or db-cAMP in the presence of HG-9–91–

01. As shown Figure 8C–E, forskolin or db-cAMP largely increased levels of the PKA substrate p-Ser157-VASP and p-CREB, however, HG-9–91–01 preferentially suppressed forskolin or db-cAMP-mediated CREB phosphorylation but not p-Ser157-VASP. These data suggest that inhibition of SIKs could downregulate cAMP-mediated CREB signaling independent of PKA. To investigate the role of SIKs in cAMP-mediated inhibition of SMC proliferation, SMCs were treated with forskolin or db-cAMP combined with HG-9–91–01. As shown in Figure 8F, HG-9–91–01, forskolin, and db-cAMP markedly suppressed cell proliferation, however, the combination of HG-9–91–01 with forskolin or with db-cAMP did not significantly change cell proliferation compared with forskolin or db-cAMP alone.

SIK inactivation-mediated CRTC3 signaling likely contributes to its anti-proliferative effect

Recent studies have demonstrated that CREB-regulated transcriptional coactivators (CRTCs) are capable of regulating CREB-targeted gene expression.[32, 33] It has been demonstrated that inactivation of SIKs can lead to CREB co-activator CRTC nuclear translocation, thereby mediating CREB signaling. To study whether SIK inactivation-mediated CRTC signaling is involved in SMC proliferation, we first examined the expression of CRTC isoforms in cultured SMCs. As shown in Figure 9A, qPCR results showed that CRTC3 was the most predominant among the three isoforms. Next, we determined the effects of SIK inhibition on CRTC3 nuclear translocation. As shown in Figure 9B–C, under both serum and serum-free conditions, CRTC3 was mainly expressed in the cytosol. However, treatment with SIK inhibitor HG-9–91–01 or MRT67307 resulted in CRTC3 translocation from the cytoplasm to nucleus, indicating that SIK inhibition can activate nuclear CRTC3 signaling. To determine whether SIK inactivation-mediated CRTC3 signaling contributes to SMC proliferation, CRTC3 siRNA was utilized. Interestingly, CRTC3 siRNA inhibited FBS-induced SMC proliferation compared with scrambled siRNA but did not further decrease the effect of HG-9–91–01 on SMC growth (Figure 9E). Consistently, CRTC3 knockdown did not alter the effect of SIK3 siRNA on SMC proliferation (Figure 9F). These data suggest that activation of CRTC3 likely contributes to SIK inhibition-mediated anti-proliferative effect on SMC proliferation.

SIK inhibition-mediated suppression of SMC proliferation is independent of HDAC4

Emerging evidence has shown that histone deacetylase 4 (HDAC4) can be regulated by SIKs in various conditions.[12, 34] HDAC4 plays a critical role in mediating SMC proliferation and neointimal formation.[12] Therefore, we proposed that HDAC4 may play a role in SIK-regulated SMC proliferation. We first examined whether SIK inhibition could alter HDAC4 expression in SMCs. As shown in Figure 10A–C, results from qPCR and western blotting revealed that HG-9–91–01 did not reduce HDAC4 expression, but conversely slightly increased its expression. Furthermore, we determined whether SIKs enabled HDAC4 intracellular trafficking. SMCs were transfected with pEGFP-HDAC4 or pEGFP-HDAC4–3SA using electroporation and then treated with HG-9–91–01. Localization of wild-type HDAC4 and the HDAC4–3SA mutant that carries mutations on phosphorylation sites necessary for nuclear export, were visualized by GFP fluorescence. As shown in Figure 10D, the transfected HDAC4-WT was predominantly expressed in the cytoplasm, and HDAC4–3SA mutant was mainly located in the nucleus. Treatment with 1 μM of HG-9–91–01 did not change the expression pattern of HDAC4 or HDAC4–3SA. Similarly, knockdown

of SIK3 did not cause HDAC4 nuclear translocation in pEGFP-HDAC4-transfected SMCs (Figure 10E). Additionally, we used the HDAC4 inhibitor MC1568 and HDAC4 siRNA to investigate whether HDAC4 plays a role in SIK inhibition-suppressed SMC proliferation. As shown in Figure 10F, we found that addition of MC1568 further decreased cell proliferation in HG-9–91–0-treated SMCs. Consistently, knockdown of HDAC4 also further decreased SMC proliferation compared with HG-9–91–01 (Figure 10G–I). These data suggest that SIK3 may regulate SMC proliferation independent of HDAC4.

Discussion

The most common adverse outcome of endovascular interventions is failure due to restenosis. Despite progress, the needs for new targets and novel therapies remain. In the present study, we investigate the role of the salt-inducible family of serine-threonine kinases in SMC migration and proliferation as related to restenosis after arterial interventions. We observed that SIK3 was highly expressed in growing SMCs and neointimal lesions of injured femoral arteries. SIK inhibition using pharmacological small molecules attenuated SMC migration and proliferation *in vitro* as well as neointima formation *in vivo*. Mechanistic studies demonstrate that SIK inactivation inhibits SMC proliferation and neointima formation through primarily down-regulation of AKT and PKA/CREB signaling.

The SIK family includes three isoforms, SIK1, SIK2, and SIK3. Although SIKs are related to the AMPK family, they appear to have distinct functions, including the ability to serve as energy sensors in all eukaryotic cell types.[12, 35] In cancer, it has been demonstrated that AMPK activation can promote human cancer cell growth and survival, and inhibiting its activity suppresses proliferation by inducing cell cycle arrest and apoptosis.[36, 37] In the vasculature, AMPK has been reported to reduce pathological vascular remodeling by mediating SMC cell cycle arrest.[38–40] By contrast, SIK3 has been demonstrated to promote cancer cell proliferation by regulating $p21^{Waf/Cip1}$ and $p27^{Kip}$.[15] However, the role of SIK3 in vascular disorders remains unknown. In this study, we used cultured SMCs that mimic synthetic SMCs in neointimal lesions, and contractile SMCs from healthy aortic media to compare the expression of three SIK isoforms. We found that SIK3 is highly expressed in cultured SMCs at a ratio of over 20 folds. It is known that SMC phenotypic modulation from a contractile to a synthetic state plays a pivotal role in cell migration, proliferation, and neointima formation.[41] Using specific SIK3 siRNA and inhibitors, we found that SIK3 could regulate neointima formation by affecting SMC proliferation. Cyclin/cyclin dependent kinase (CKD) complex-mediated G1-S progression of the cell cycle is critical for SMC proliferation.[42] Cyclin-dependent kinase inhibitors such as p27Kip1 and p21Cip1 can negatively control cyclin/CDK complexes. Numerous drugs have been found to inhibit SMC proliferation through p27Kip1 and p21Cip-mediated cell cycle arrest. For example, sirolimus and paclitaxel that are used to coat stents can lead to cell cycle arrest by up-regulating p27Kip1 and p21Cip1.[43, 44] It has been reported that SIK3 is able to regulate cell cycle progression in cancer cells while knockdown of SIK3 increases the mitotic index in HeLa and H1299.[16] In this study, we report that the SIK inhibitor HG-9–91–01 was able to block G_1/S transition by up-regulating cyclin B1, D1 and E1 in SMCs (Figure 3). The underlying mechanisms may involve up-regulating p27Kip1 and p21Cip1.

It has been well demonstrated that AKT and ERK1/2 signaling play critical roles in SMC migration and proliferation, as well as pathological vascular remodeling.[21, 28] The differential effects targeting AKT and ERK1/2 signaling have also been reported. For example, vinpocetine, a PDE1 inhibitor, can suppress PDGF-BB-induced phosphorylation of ERK1/2 but not AKT in rat aortic SMCs.[21] Nitric oxide inhibits PDGF-induced activation of AKT but not ERK1/2 in A7r5 cells.[45] In this study, we found that SIK inhibition using HG-9–91–01 was able to block FBS-induced phosphorylation of AKT but not ERK1/2 (Figure 6). Previous studies demonstrated that the cAMP responsive element-binding protein (CREB) could promote cell proliferation in arterial SMCs and cancer cells.[46, 47] Recent studies also showed that activating PKA/CREB signaling was critical for SMC proliferation.[29] In this study, we found that SIK inhibition attenuated FBS-induced PKA/CREB signaling, showing increased CREB phosphorylation and pSer157 VASP, a PKA substrate, in SMCs. Using small molecule inhibitors of PKA and CREB, we observed that inhibition of PKA or CREB dose-dependently suppressed FBS-mediated SMC proliferation. This is consistent with the recent study showing that growth factor-activated CREB had a pro-mitogenic effect, which was p-Ser133-dependent.[48] Previous studies also demonstrated that CREB could be activated by various kinases including AKT.[49, 50] Therefore, it is possible that SIK inhibition suppresses SMC proliferation by blocking the AKT/CREB signaling pathway. Interestingly, when we used CREB siRNA to further validate the effect of CREB signaling on SMC proliferation, we surprisingly observed that knockdown of CREB did not abrogate FBS-induced cell proliferation. On the contrary, it facilitated FBS-mediated cell proliferation. CREB knockdown also increased cell proliferation in HG-9–91–0-treated SMCs. This discrepancy could be due to the dual roles of CREB. CREB can transcriptionally increase or suppress large number of genes, thereby regulating numerous pathophysiological events. For example, CREB could serve as a gatekeeper for preventing transition of SMC from a contractile to a synthetic phenotype. Loss of CREB in rodent models is a permissive step for SMC activation.[51] Similarly, other investigators have also demonstrated that knockdown of CREB promoted cell proliferation in various cell lines including KMH2, L1236, L428, HDLM2, and L540 cells.[52] These data suggest that CREB phosphorlation and CREB expression could play different roles in cell proliferation. Moreover, it is well known that the phosphorlation of CREB at Ser133 is capable of inhibiting SMC proliferation and phenotypic modulation. Our data showed that under cAMP stimulation, CREB signaling exhibits an anti-proliferative effect, while in growth factor-stimulation, it has a pro-proliferative action. These data suggest that CREB plays dual roles in regulating cell proliferation.

It is known that cAMP/PKA activation could be regulated by upstream signaling factors such as the G-protein-coupled receptor (GPCR) family, adenylyl cyclases (ACs), and various phosphodiesterase (PDE) family members..[53–55] Numerous studies have demonstrated that activating cAMP/PKA signaling can inhibit SMC proliferation.[17, 30, 31] In the present study, we found that cAMP/PKA signaling induced by the adenylyl cyclase activator forskolin or cAMP analog db-cAMP suppressed FBS-mediated SMC proliferation, and that SIK inhibition antagonized forskolin- or db-cAMP-induced CREB phosphorylation but not PKA activation, suggesting that inhibition of SIKs could down-regulate cAMP-mediated CREB signaling independent of PKA. However, when we investigated the role of SIKs

in cAMP-suppressed SMC proliferation, we found that SIK inhibition failed to block cAMP-inhibited cell proliferation. This discrepancy could be due to the anti-proliferative effects of SIK inhibition via suppression of AKT signaling, which could counteract the effect of SIK inhibition on cAMP signaling-mediated anti-proliferative effects. However, the detailed mechanisms need further investigation. Emerging evidence suggests that CREB plays a critical role in regulating downstream gene expression through its co-activator CRTCs.[32, 56] Under basal conditions, CRTCs are phosphorylated by SIKs and sequestered via interaction with 13–3–3 protein in the cytoplasm. Elevated cAMP levels can inhibit SIK activity, resulting in CRTC dephosphorylation and nuclear translocation that promote CREB targeted gene expression.[32, 57] It has been demonstrated that CRTC-mediated regulation of CREB is associated with many human processes including cardiovascular disease, insulin sensitivity, and lipid metabolism.[30, 33, 58, 59] We observed that CRTC3 was primarily distributed in the cytoplasm of FBS-stimulated SMCs, and that SIK inhibition by HG-9–91–01 resulted in CRTC3 nuclear translocation. We also found that knockdown of CRTC3 suppressed FBS-mediated SMC proliferation but did not further decrease SMC proliferation compared with SIK inhibition or SIK3 knockdown. These data suggest that CRTC3 nuclear signaling could contribute, at least partially, to SIK inactivation-mediated inhibition of SMC proliferation. Similarly, a recent study has also demonstrated that activation of CRTC2/3 signaling could suppress cAMP-induced inhibition of proliferation.[48] In the present study, we also observed that the cAMP activator forskolin could mediate CRTC3 nuclear translocation (Figure 9D). It is known that cAMP can inhibit SIKs. Therefore, we suggest that cAMP-triggered CRTC3 activation could also contribute to its anti-proliferative effect. It has been also demonstrated that class IIα HDAC4 plays an important role in mediating SMC proliferation. Previous studies showed that inhibition of HDAC4 suppressed arterial injury-induced neointima formation as well as SMC proliferation.[60, 61] Increased evidence also suggests that SIKs are capable of regulating HDAC4. Similar to CRTCs, HDAC4 can translocate to the nucleus from the cytoplasm following dephosphorylation and thereby regulate gene expression.[62] It has been demonstrated that SIK-mediated regulation of HDAC4 plays important roles in various pathophysiological processes including lipid metabolism and vascular calcification.[34, 62, 63] However, our data showed that although inhibition or knockdown of HDAC4 suppressed FBS-induced SMC proliferation, it was unlikely involved in SIK inactivation-mediated inhibition of SMC proliferation.

In summary, we have demonstrated that SIK3 is highly expressed in cultured SMCs as well as neointimal lesions after arterial injury. Inhibition of SIKs using small molecule inhibitors suppresses SMC proliferation *in vitro*, as well as decreases neointima formation after arterial injury *in vivo*. The underlying mechanisms whereby SIKs regulate arterial restenosis could primarily involve AKT and PKA/CREB signaling. CRTC3 activation could, at least partially, contribute to SIK inhibition-mediated anti-proliferative effect. Our data provides insights into the potential for targeting SIKs as a therapeutic strategy for slowing restenosis in patients with vascular interventions.

Supplementary Material

Refer to Web version on PubMed Central for supplementary material.

Sources of Funding

This work was supported by AHA/Scientist Development Grant 13SDG16560024 (Y.C), AHA/Transformational Project Award 19TPA34830071 (Y.C.) and NIH grants R01HL138357 and R01HL105641 (R.G.)

Non-standard Abbreviations and Acronyms:

NBF	10% phosphate-buffered formalin
H&E	hematoxylin and eosin
VVG	Verhoeff-Van Gieson
DMEM	Dulbecco's modified eagle's medium
GAPDH	glyceraldehyde-3-phosphate dehydrogenase
PFA	4% paraformaldehyde
SMCs	vascular smooth muscle cells
SIK	salt-inducible kinase
AMPK	AMP-activated protein kinase
MAPK	mitogen-activated protein kinase
PKA	protein kinase A
CREB	cAMP response element-binding protein
FBS	fetal bovine serum
LKB1	liver kinase B1
PCNA	proliferating cell nuclear antigen
SM-MHC	smooth muscle myosin heavy chain
AKT	protein kinase B
Erk	extracellular signal-regulated protein kinase
VASP	vasodilator-stimulated phosphoprotein
CRTC	CREB-regulated transcriptional coactivator
HDAC4	histone deacetylase 4
CKD	cyclin dependent kinase
GPCR	G-protein-coupled receptor
PDE	phosphodiesterase
AC	adenylyl cyclase

References

1. Thukkani AK and Kinlay S. Endovascular intervention for peripheral artery disease. Circ Res. 2015;116:1599–613. [PubMed: 25908731]
2. Schillinger M, Sabeti S, Loewe C, Dick P, Amighi J, Mlekusch W, Schlager O, Cejna M, Lammer J and Minar E. Balloon angioplasty versus implantation of nitinol stents in the superficial femoral artery. N Engl J Med. 2006;354:1879–88. [PubMed: 16672699]
3. Owens GK, Kumar MS and Wamhoff BR. Molecular regulation of vascular smooth muscle cell differentiation in development and disease. Physiol Rev. 2004;84:767–801. [PubMed: 15269336]
4. Regan CP, Adam PJ, Madsen CS and Owens GK. Molecular mechanisms of decreased smooth muscle differentiation marker expression after vascular injury. J Clin Invest. 2000;106:1139–47. [PubMed: 11067866]
5. Jukema JW, Verschuren JJ, Ahmed TA and Quax PH. Restenosis after PCI. Part 1: pathophysiology and risk factors. Nat Rev Cardiol. 2012;9:53–62.
6. Schober A and Zernecke A. Chemokines in vascular remodeling. Thromb Haemost. 2007;97:730–7. [PubMed: 17479183]
7. Rensen SS, Doevendans PA and van Eys GJ. Regulation and characteristics of vascular smooth muscle cell phenotypic diversity. Neth Heart J. 2007;15:100–8. [PubMed: 17612668]
8. Wein MN, Foretz M, Fisher DE, Xavier RJ and Kronenberg HM. Salt-Inducible Kinases: Physiology, Regulation by cAMP, and Therapeutic Potential: (Trends Endocrinol. Metab. 29, 723–735, 2018). Trends Endocrinol Metab. 2019;30:407. [PubMed: 30837108]
9. Grubbs JJ, Lopes LE, van der Linden AM and Raizen DM. A salt-induced kinase is required for the metabolic regulation of sleep. PLoS Biol. 2020;18:e3000220. [PubMed: 32315298]
10. Uebi T, Itoh Y, Hatano O, Kumagai A, Sanosaka M, Sasaki T, Sasagawa S, Doi J, Tatsumi K, Mitamura K, Morii E, Aozasa K, Kawamura T, Okumura M, Nakae J, Takikawa H, Fukusato T, Koura M, Nish M, Hamsten A, Silveira A, Bertorello AM, Kitagawa K, Nagaoka Y, Kawahara H, Tomonaga T, Naka T, Ikegawa S, Tsumaki N, Matsuda J and Takemori H. Involvement of SIK3 in glucose and lipid homeostasis in mice. PLoS One. 2012;7:e37803. [PubMed: 22662228]
11. Bertorello AM, Pires N, Igreja B, Pinho MJ, Vorkapic E, Wagsater D, Wikstrom J, Behrendt M, Hamsten A, Eriksson P, Soares-da-Silva P and Brion L. Increased arterial blood pressure and vascular remodeling in mice lacking salt-inducible kinase 1 (SIK1). Circ Res. 2015;116:642–52. [PubMed: 25556206]
12. Sakamoto K, Bultot L and Goransson O. The Salt-Inducible Kinases: Emerging Metabolic Regulators. Trends Endocrinol Metab. 2018;29:827–840. [PubMed: 30385008]
13. Cheng H, Liu P, Wang ZC, Zou L, Santiago S, Garbitt V, Gjoerup OV, Iglehart JD, Miron A, Richardson AL, Hahn WC and Zhao JJ. SIK1 couples LKB1 to p53-dependent anoikis and suppresses metastasis. Sci Signal. 2009;2:ra35. [PubMed: 19622832]
14. Zohrap N, Saatci O, Ozes B, Coban I, Atay HM, Battaloglu E, Sahin O and Bugra K. SIK2 attenuates proliferation and survival of breast cancer cells with simultaneous perturbation of MAPK and PI3K/Akt pathways. Oncotarget. 2018;9:21876–21892. [PubMed: 29774109]
15. Charoenfuprasert S, Yang YY, Lee YC, Chao KC, Chu PY, Lai CR, Hsu KF, Chang KC, Chen YC, Chen LT, Chang JY, Leu SJ and Shih NY. Identification of salt-inducible kinase 3 as a novel tumor antigen associated with tumorigenesis of ovarian cancer. Oncogene. 2011;30:3570–84. [PubMed: 21399663]
16. Chen H, Huang S, Han X, Zhang J, Shan C, Tsang YH, Ma HT and Poon RY. Salt-inducible kinase 3 is a novel mitotic regulator and a target for enhancing antimitotic therapeutic-mediated cell death. Cell Death Dis. 2014;5:e1177. [PubMed: 24743732]
17. Cai Y, Nagel DJ, Zhou Q, Cygnar KD, Zhao H, Li F, Pi X, Knight PA and Yan C. Role of cAMP-phosphodiesterase 1C signaling in regulating growth factor receptor stability, vascular smooth muscle cell growth, migration, and neointimal hyperplasia. Circ Res. 2015;116:1120–32. [PubMed: 25608528]
18. Sata M, Maejima Y, Adachi F, Fukino K, Saiura A, Sugiura S, Aoyagi T, Imai Y, Kurihara H, Kimura K, Omata M, Makuuchi M, Hirata Y and Nagai R. A mouse model of vascular injury that

induces rapid onset of medial cell apoptosis followed by reproducible neointimal hyperplasia. J Mol Cell Cardiol. 2000;32:2097–104. [PubMed: 11040113]

19. Sreejayan N and Yang X. Isolation and functional studies of rat aortic smooth muscle cells. Methods Mol Med. 2007;139:283–92. [PubMed: 18287680]
20. Orellana EA and Kasinski AL. Sulforhodamine B (SRB) Assay in Cell Culture to Investigate Cell Proliferation. Bio Protoc. 2016;6.
21. Cai Y, Knight WE, Guo S, Li JD, Knight PA and Yan C. Vinpocetine suppresses pathological vascular remodeling by inhibiting vascular smooth muscle cell proliferation and migration. J Pharmacol Exp Ther. 2012;343:479–88. [PubMed: 22915768]
22. Liang CC, Park AY and Guan JL. In vitro scratch assay: a convenient and inexpensive method for analysis of cell migration in vitro. Nat Protoc. 2007;2:329–33. [PubMed: 17406593]
23. Filippov S, Koenig GC, Chun TH, Hotary KB, Ota I, Bugge TH, Roberts JD, Fay WP, Birkedal-Hansen H, Holmbeck K, Sabeh F, Allen ED and Weiss SJ. MT1-matrix metalloproteinase directs arterial wall invasion and neointima formation by vascular smooth muscle cells. J Exp Med. 2005;202:663–71. [PubMed: 16147977]
24. Pozarowski P and Darzynkiewicz Z. Analysis of cell cycle by flow cytometry. Methods Mol Biol. 2004;281:301–11. [PubMed: 15220539]
25. Basi DL, Adhikari N, Mariash A, Li Q, Kao E, Mullegama SV and Hall JL. Femoral artery neointimal hyperplasia is reduced after wire injury in Ref-1+/− mice. Am J Physiol Heart Circ Physiol. 2007;292:H516–21. [PubMed: 16936011]
26. Tang DD and Gerlach BD. The roles and regulation of the actin cytoskeleton, intermediate filaments and microtubules in smooth muscle cell migration. Respir Res. 2017;18:54. [PubMed: 28390425]
27. Gerthoffer WT. Mechanisms of vascular smooth muscle cell migration. Circ Res. 2007;100:607–21. [PubMed: 17363707]
28. Deuse T, Koyanagi T, Erben RG, Hua X, Velden J, Ikeno F, Reichenspurner H, Robbins RC, Mochly-Rosen D and Schrepfer S. Sustained inhibition of epsilon protein kinase C inhibits vascular restenosis after balloon injury and stenting. Circulation. 2010;122:S170–8. [PubMed: 20837910]
29. Rondeau V, Jain A, Truong V and Srivastava AK. Involvement of the Akt-dependent CREB signaling pathway in hydrogen-peroxide-induced early growth response protein-1 expression in rat vascular smooth muscle cells (1). Can J Physiol Pharmacol. 2019;97:885–892. [PubMed: 30939252]
30. Chen WJ, Chen YH, Lin KH, Ting CH and Yeh YH. Cilostazol promotes vascular smooth muscles cell differentiation through the cAMP response element-binding protein-dependent pathway. Arterioscler Thromb Vasc Biol. 2011;31:2106–13. [PubMed: 21680899]
31. Fukumoto S, Koyama H, Hosoi M, Yamakawa K, Tanaka S, Morii H and Nishizawa Y. Distinct role of cAMP and cGMP in the cell cycle control of vascular smooth muscle cells: cGMP delays cell cycle transition through suppression of cyclin D1 and cyclin-dependent kinase 4 activation. Circ Res. 1999;85:985–91. [PubMed: 10571528]
32. Altarejos JY and Montminy M. CREB and the CRTC co-activators: sensors for hormonal and metabolic signals. Nat Rev Mol Cell Biol. 2011;12:141–51. [PubMed: 21346730]
33. MacKenzie KF, Clark K, Naqvi S, McGuire VA, Noehren G, Kristariyanto Y, van den Bosch M, Mudaliar M, McCarthy PC, Pattison MJ, Pedrioli PG, Barton GJ, Toth R, Prescott A and Arthur JS. PGE(2) induces macrophage IL-10 production and a regulatory-like phenotype via a protein kinase A-SIK-CRTC3 pathway. J Immunol. 2013;190:565–77. [PubMed: 23241891]
34. Abend A, Shkedi O, Fertouk M, Caspi LH and Kehat I. Salt-inducible kinase induces cytoplasmic histone deacetylase 4 to promote vascular calcification. EMBO Rep. 2017;18:1166–1185. [PubMed: 28588072]
35. Hardie DG, Carling D and Carlson M. The AMP-activated/SNF1 protein kinase subfamily: metabolic sensors of the eukaryotic cell? Annu Rev Biochem. 1998;67:821–55. [PubMed: 9759505]

36. Hu M, Chen X, Ma L, Ma Y, Li Y, Song H, Xu J, Zhou L, Li X, Jiang Y, Kong B and Huang P. AMPK Inhibition Suppresses the Malignant Phenotype of Pancreatic Cancer Cells in Part by Attenuating Aerobic Glycolysis. J Cancer. 2019;10:1870–1878. [PubMed: 31205544]
37. Park HU, Suy S, Danner M, Dailey V, Zhang Y, Li H, Hyduke DR, Collins BT, Gagnon G, Kallakury B, Kumar D, Brown ML, Fornace A, Dritschilo A and Collins SP. AMP-activated protein kinase promotes human prostate cancer cell growth and survival. Mol Cancer Ther. 2009;8:733–41. [PubMed: 19372545]
38. Stone JD, Narine A, Shaver PR, Fox JC, Vuncannon JR and Tulis DA. AMP-activated protein kinase inhibits vascular smooth muscle cell proliferation and migration and vascular remodeling following injury. Am J Physiol Heart Circ Physiol. 2013;304:H369–81. [PubMed: 23203966]
39. Nagata D, Takeda R, Sata M, Satonaka H, Suzuki E, Nagano T and Hirata Y. AMP-activated protein kinase inhibits angiotensin II-stimulated vascular smooth muscle cell proliferation. Circulation. 2004;110:444–51. [PubMed: 15262850]
40. Igata M, Motoshima H, Tsuruzoe K, Kojima K, Matsumura T, Kondo T, Taguchi T, Nakamaru K, Yano M, Kukidome D, Matsumoto K, Toyonaga T, Asano T, Nishikawa T and Araki E. Adenosine monophosphate-activated protein kinase suppresses vascular smooth muscle cell proliferation through the inhibition of cell cycle progression. Circ Res. 2005;97:837–44. [PubMed: 16151020]
41. Nguyen AT, Gomez D, Bell RD, Campbell JH, Clowes AW, Gabbiani G, Giachelli CM, Parmacek MS, Raines EW, Rusch NJ, Speer MY, Sturek M, Thyberg J, Towler DA, Weiser-Evans MC, Yan C, Miano JM and Owens GK. Smooth muscle cell plasticity: fact or fiction? Circ Res. 2013;112:17–22. [PubMed: 23093573]
42. Braun-Dullaeus RC, Mann MJ and Dzau VJ. Cell cycle progression: new therapeutic target for vascular proliferative disease. Circulation. 1998;98:82–9. [PubMed: 9665064]
43. Moses JW, Leon MB, Popma JJ, Fitzgerald PJ, Holmes DR, O'Shaughnessy C, Caputo RP, Kereiakes DJ, Williams DO, Teirstein PS, Jaeger JL and Kuntz RE. Sirolimus-eluting stents versus standard stents in patients with stenosis in a native coronary artery. N Engl J Med. 2003;349:1315–23. [PubMed: 14523139]
44. Stone GW, Ellis SG, Cox DA, Hermiller J, O'Shaughnessy C, Mann JT, Turco M, Caputo R, Bergin P, Greenberg J, Popma JJ and Russell ME. A polymer-based, paclitaxel-eluting stent in patients with coronary artery disease. N Engl J Med. 2004;350:221–31. [PubMed: 14724301]
45. Sandirasegarane L, Charles R, Bourbon N and Kester M. NO regulates PDGF-induced activation of PKB but not ERK in A7r5 cells: implications for vascular growth arrest. Am J Physiol Cell Physiol. 2000;279:C225–35. [PubMed: 10898734]
46. Jalvy S, Renault MA, Lam Shang Leen L, Belloc I, Reynaud A, Gadeau AP and Desgranges C. CREB mediates UTP-directed arterial smooth muscle cell migration and expression of the chemotactic protein osteopontin via its interaction with activator protein-1 sites. Circ Res. 2007;100:1292–9. [PubMed: 17413042]
47. Sakamoto KM and Frank DA. CREB in the pathophysiology of cancer: implications for targeting transcription factors for cancer therapy. Clin Cancer Res. 2009;15:2583–7. [PubMed: 19351775]
48. Hudson C, Kimura TE, Duggirala A, Sala-Newby GB, Newby AC and Bond M. Dual Role of CREB in The Regulation of VSMC Proliferation: Mode of Activation Determines Pro- or Anti-Mitogenic Function. Sci Rep. 2018;8:4904. [PubMed: 29559698]
49. Du K and Montminy M. CREB is a regulatory target for the protein kinase Akt/PKB. J Biol Chem. 1998;273:32377–9. [PubMed: 9829964]
50. Zhu M, Zheng R, Guo Y, Zhang Y and Zuo B. NDRG4 promotes myogenesis via Akt/CREB activation. Oncotarget. 2017;8:101720–101734. [PubMed: 29254199]
51. Reusch JE and Klemm DJ. Cyclic AMP response element-binding protein in the vessel wall: good or bad? Circulation. 2003;108:1164–6. [PubMed: 12963681]
52. Lu F, Zheng Y, Donkor PO, Zou P and Mu P. Downregulation of CREB Promotes Cell Proliferation by Mediating G1/S Phase Transition in Hodgkin Lymphoma. Oncol Res. 2016;24:171–9. [PubMed: 27458098]
53. Tilley DG. G protein-dependent and G protein-independent signaling pathways and their impact on cardiac function. Circ Res. 2011;109:217–30. [PubMed: 21737817]

54. Cooper DM. Regulation and organization of adenylyl cyclases and cAMP. Biochem J. 2003;375:517–29. [PubMed: 12940771]
55. Bender AT and Beavo JA. Cyclic nucleotide phosphodiesterases: molecular regulation to clinical use. Pharmacol Rev. 2006;58:488–520. [PubMed: 16968949]
56. Takahashi N, Tetsuka T, Uranishi H and Okamoto T. Inhibition of the NF-kappaB transcriptional activity by protein kinase A. Eur J Biochem. 2002;269:4559–65. [PubMed: 12230568]
57. Luan B, Goodarzi MO, Phillips NG, Guo X, Chen YD, Yao J, Allison M, Rotter JI, Shaw R and Montminy M. Leptin-mediated increases in catecholamine signaling reduce adipose tissue inflammation via activation of macrophage HDAC4. Cell Metab. 2014;19:1058–65. [PubMed: 24768298]
58. Fang WL, Lee MT, Wu LS, Chen YJ, Mason J, Ke FC and Hwang JJ. CREB coactivator CRTC2/TORC2 and its regulator calcineurin crucially mediate follicle-stimulating hormone and transforming growth factor beta1 upregulation of steroidogenesis. J Cell Physiol. 2012;227:2430–40. [PubMed: 21826657]
59. Mair W, Morantte I, Rodrigues AP, Manning G, Montminy M, Shaw RJ and Dillin A. Lifespan extension induced by AMPK and calcineurin is mediated by CRTC-1 and CREB. Nature. 2011;470:404–8. [PubMed: 21331044]
60. Usui T, Morita T, Okada M and Yamawaki H. Histone deacetylase 4 controls neointimal hyperplasia via stimulating proliferation and migration of vascular smooth muscle cells. Hypertension. 2014;63:397–403. [PubMed: 24166750]
61. Zheng X, Wu Z, Xu K, Qiu Y, Su X, Zhang Z and Zhou M. Interfering histone deacetylase 4 inhibits the proliferation of vascular smooth muscle cells via regulating MEG3/miR-125a-5p/IRF1. Cell Adh Migr. 2019;13:41–49. [PubMed: 30156956]
62. Henriksson E, Sall J, Gormand A, Wasserstrom S, Morrice NA, Fritzen AM, Foretz M, Campbell DG, Sakamoto K, Ekelund M, Degerman E, Stenkula KG and Goransson O. SIK2 regulates CRTCs, HDAC4 and glucose uptake in adipocytes. J Cell Sci. 2015;128:472–86. [PubMed: 25472719]
63. Fujii S, Emery P and Amrein H. SIK3-HDAC4 signaling regulates Drosophila circadian male sex drive rhythm via modulating the DN1 clock neurons. Proc Natl Acad Sci U S A. 2017;114:E6669–E6677. [PubMed: 28743754]

Highlights

- SIK3 is highly expressed in proliferating SMCs, and decreasing SIK3 levels or activity reduces SMC proliferation *in vitro* and *in vivo*.
- SIK inactivation suppresses SMC proliferation by inhibiting AKT signaling and by down-regulating PKA-CREB signaling.
- SIK inhibition-mediated CRTC3 signaling likely contributes to its anti-proliferative effects.

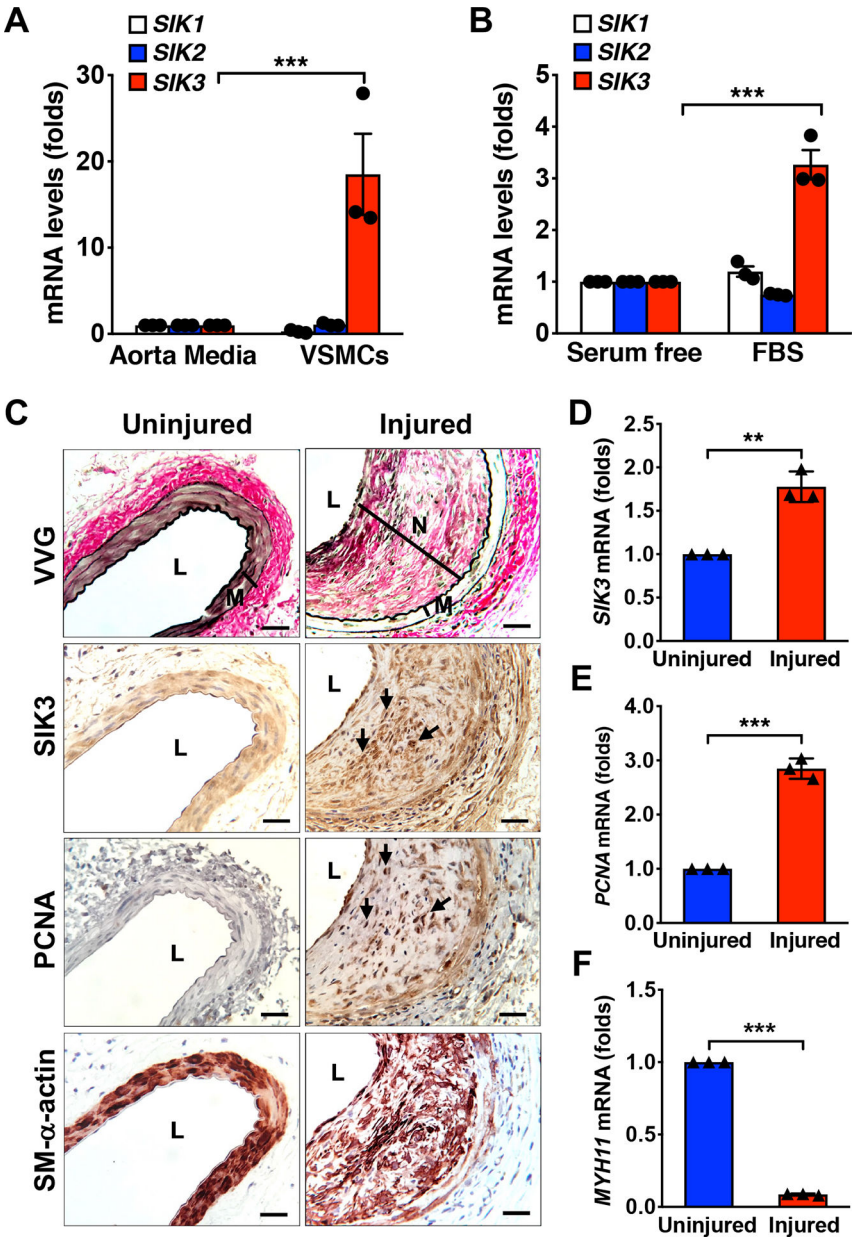

Figure 1. SIK3 is highly expressed in growing SMCs *in vitro* as well as neointimal lesions *in vivo*.

A. qPCR data showing mRNA levels of SIKs in growing and contractile SMCs. Contractile SMCs (normal aortic medial SMCs) were isolated from rat aortic media by peeling off the adventitia and scraping the endothelial layer. Synthetic SMCs (cultured aortic SMCs) were obtained from corresponding aortic media using an explant method. **B**. Effects of FBS on mRNA levels of SIKs in SMCs. Rat aortic SMCs were starved and then stimulated with 5% FBS for 24 h. **C**. Representative immunohistochemistry images showing the expression of SIK3 and PCNA (a proliferation marker), and SM-α-actin (a SMC marker) in injured and uninjured arteries in mice. Arterial injury was induced using a femoral artery wire injury procedure. Left femoral artery was injured to induce neointima formation. Right femoral artery was uninjured control. Elastin fiber was stained using VVG method. **D–F**. qPCR data

showing mRNA expression of SIK3, PCNA, and MYH11 (a SMC contractile marker) in injured and uninjured arteries. qPCR results were normalized using GAPDH. Data were analyzed by t-test. Values are mean ± SD (n=3). $^{**}P < 0.01$, $^{***}P < 0.001$. N, neointima; M, media; L, lumen. Arrow, SIK3 positive or PCNA positive staining. Scale bar, 25 μm.

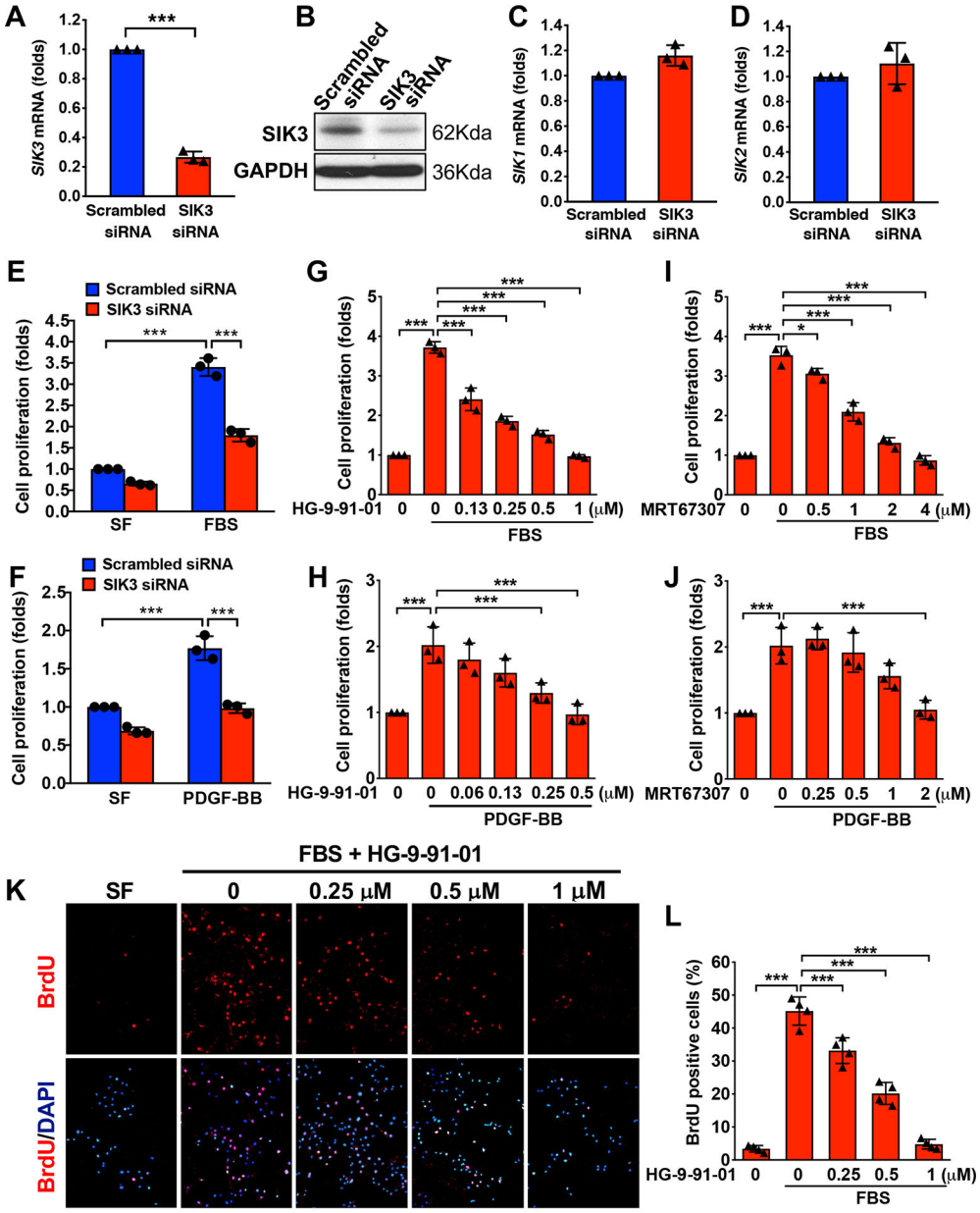

Figure 2. Knockdown and inhibition of SIK3 suppress SMC proliferation *in vitro*.

A-D. Knockdown of SIK3 specific decreased SIK3 without affecting SIK1 and SIK2 in SMCs. mRNA and protein levels of SIK3 were determined by qPCR and western blotting, respectively (**A-B**), and mRNA expression of SIK1 and SIK2 was examined by qPCR (**C-D**). **E-F**. Effects of SIK3 knockdown on SMC proliferation. Rat aortic SMCs were transfected with 100 nM scrambled siRNA or SIK3 siRNA, and then serum-free (SF) starved, followed by stimulation with 5% FBS or 50 ng/ml PDGF-BB for 48 h. **G-J**. Effects of SIK inhibition on SMC proliferation. Rat aortic SMCs were serum-free starved and then treated with SIK inhibitors HG-9–91–01 or MRT67307 for 0.5 h, followed by stimulated with 5% FBS or 50 ng/ml PDGF-BB for 48 h. Cell proliferation was measured by SRB assay. **K**. Representative immunofluorescence images showing the effects of HG-9–

91–01 on SMC proliferation. **L**. Quantitative results of immunofluorescence staining. Rat aortic SMCs were serum-free (SF) starved and then treated with HG-9–91–01, followed by stimulation with 5% FBS for 24 h. 40 μM of BrdU was added at 2.5 h before harvesting cells. The proliferative cells were stained with BrdU antibody. Nuclei were stained with DAPI. Data were analyzed by t-test, one-way ANOVA or two-way ANOVA with multiple comparisons. ANOVA analysis was corrected with post hoc test. Values are mean ± SD (n=3–4). $*P < 0.05$, $***P < 0.001$.

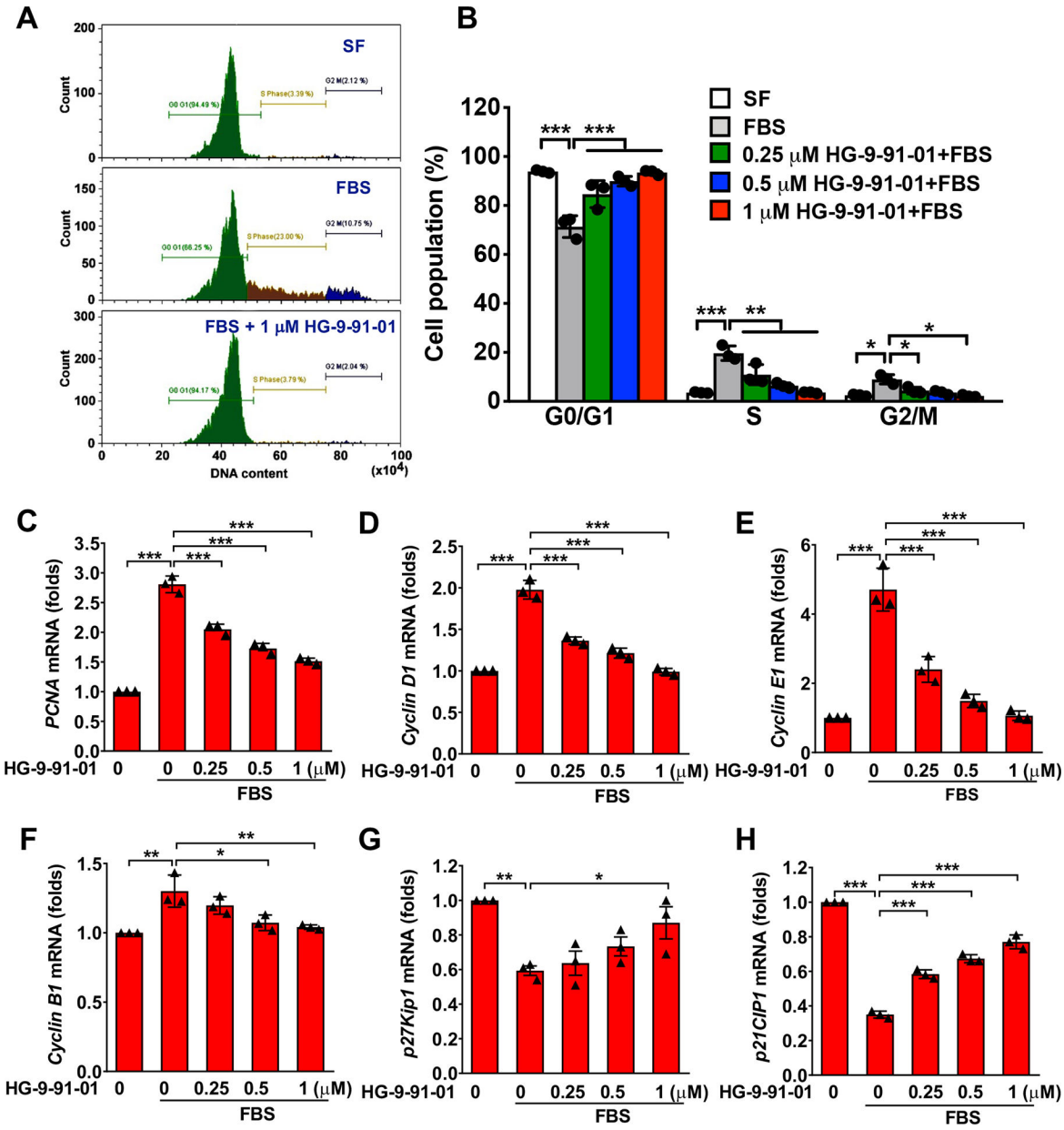

Figure 3. SIK inhibition suppresses SMC proliferation and up-regulates p21^{CIP1} and p27^{KIP1}.

A. Representative flow cytometry analysis showing the effects of SIK inhibition on cell cycle. Rat aortic SMCs were serum-free (SF) starved and then treated with SIK inhibitor HG-9–91–01 for 0.5 h, followed by stimulated with 5% FBS for 24 h. Cell cycle was assessed using flow cytometry. **B**. Quantitative results of flow cytometry analysis. **C**-**H**. qPCR data showing the effects of SIK inhibitor on expression of PCNA, cyclin D, E1 and B1, p21^{CIP1} and p27^{KIP1} during SMC proliferation. Rat aortic SMCs were serum-free starved and then treated with SIK inhibitor HG-9–91–01 for 0.5 h, followed by stimulated with 5% FBS for 18 h. Levels of mRNA were examined using qPCR. Results were normalized using GAPDH. Data were analyzed by one-way ANOVA or two-way ANOVA

with multiple comparisons. ANOVA analysis was corrected with post hoc test. Values are mean ± SD (n=3). *$P < 0.05$, **$P < 0.01$, ***$P < 0.001$.

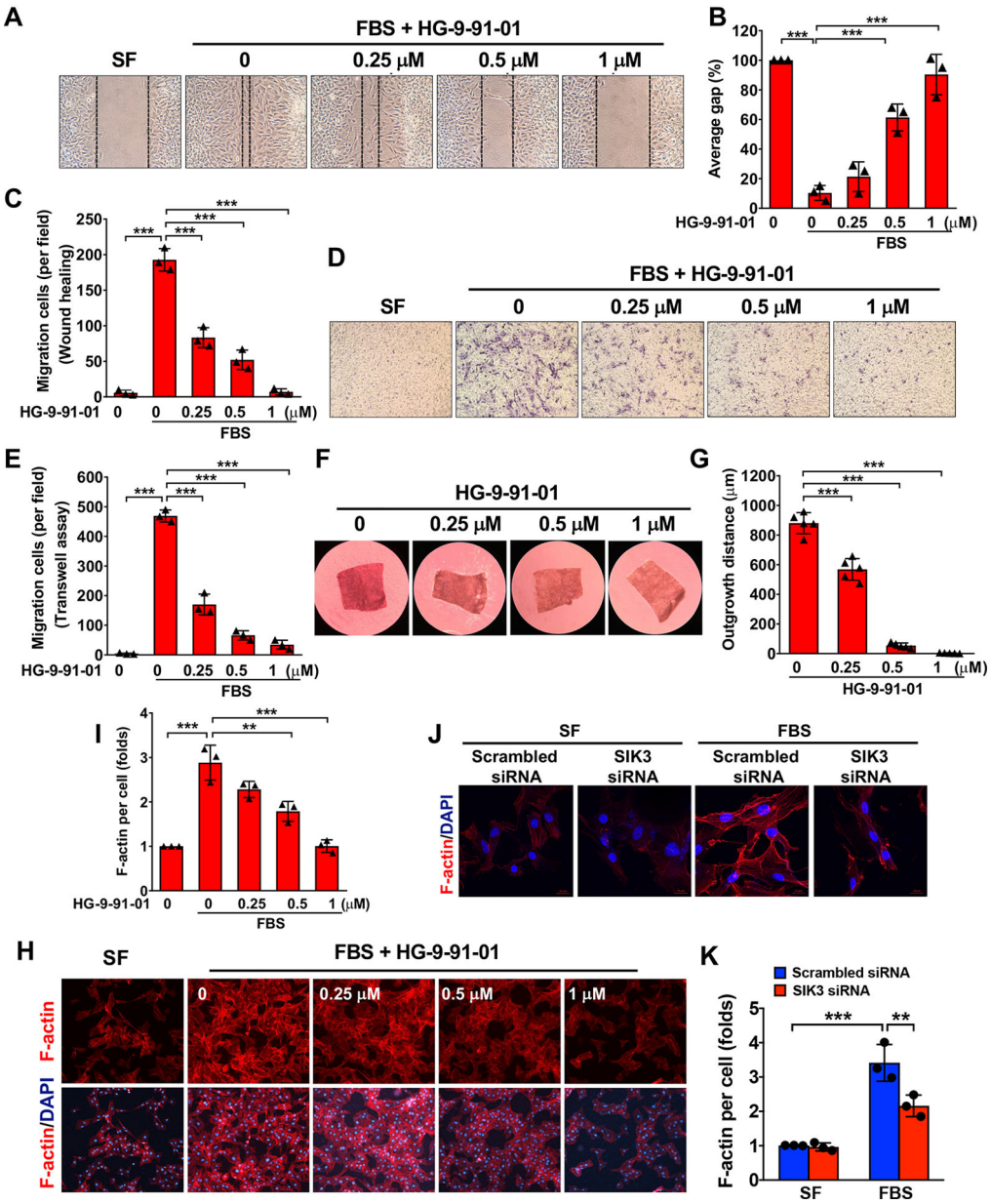

Figure 4. SIK inactivation attenuates SMC migration and modulates actin polymerization.

A. Representative images from the wound-healing assay showing the effects of SIK inhibition on SMC migration. **B-C**. Quantitative results of wound-healing assay. Confluent rat aortic SMCs in 35 mm dishes were serum-free starved then treated with SIK inhibitor HG-9–91–01 for 0.5 h, followed by stimulated with 5% FBS for 6 h. **D**. Representative images from the modified Boyden chamber assay showing the effects of SIK inhibition on SMC migration. **E**. Quantitative data of modified Boyden chamber assay. Rat aortic SMCs seeded in Transwells in a 24-well plate were treated with SIK inhibitor HG-9–91–01 for 0.5 h and then stimulated with 5% FBS for 6 h. **F**. Representative images showing the effects of HG-9–91–01 on growth factors-induced SMC outgrowth *ex vivo*. Aortic media explants were embedded in a type I collagen 3D gel and treated with HG-9–91-01, followed

by stimulation with 10 ng/ml PDGF-BB and 10 ng/ml FGF2 for 10 days. **G**. Quantitative results from 3D culture system *ex vivo*. **H**. Representative immunofluorescence images showing the effects of SIK inhibition on FBS-induced actin polymerization. Rat aortic SMCs were serum-free starved and then treated with SIK inhibitor HG-9–91–01 for 0.5 h, followed by stimulation with 5% FBS for 24 h. **I**. Quantitative results of F-actin cytoskeleton immunostaining. **J**-**K**. Effects of SIK3 knockdown on FBS-induced actin polymerization. Rat aortic SMCs were transfected with 100 nM scrambled siRNA or SIK3 siRNA, and then serum-free starved, followed by stimulation with 5% FBS for 24 h. F-actin cytoskeleton was immunostained using Phalloidin CruzFluor™ 594 Conjugate. Nuclei were stained with DAPI. Data were analyzed by one-way ANOVA or two-way ANOVA with multiple comparisons. ANOVA analysis was corrected with post hoc test. Values are mean ± SD. n=3–5. $^{**}P < 0.01$, $^{***}P < 0.001$.

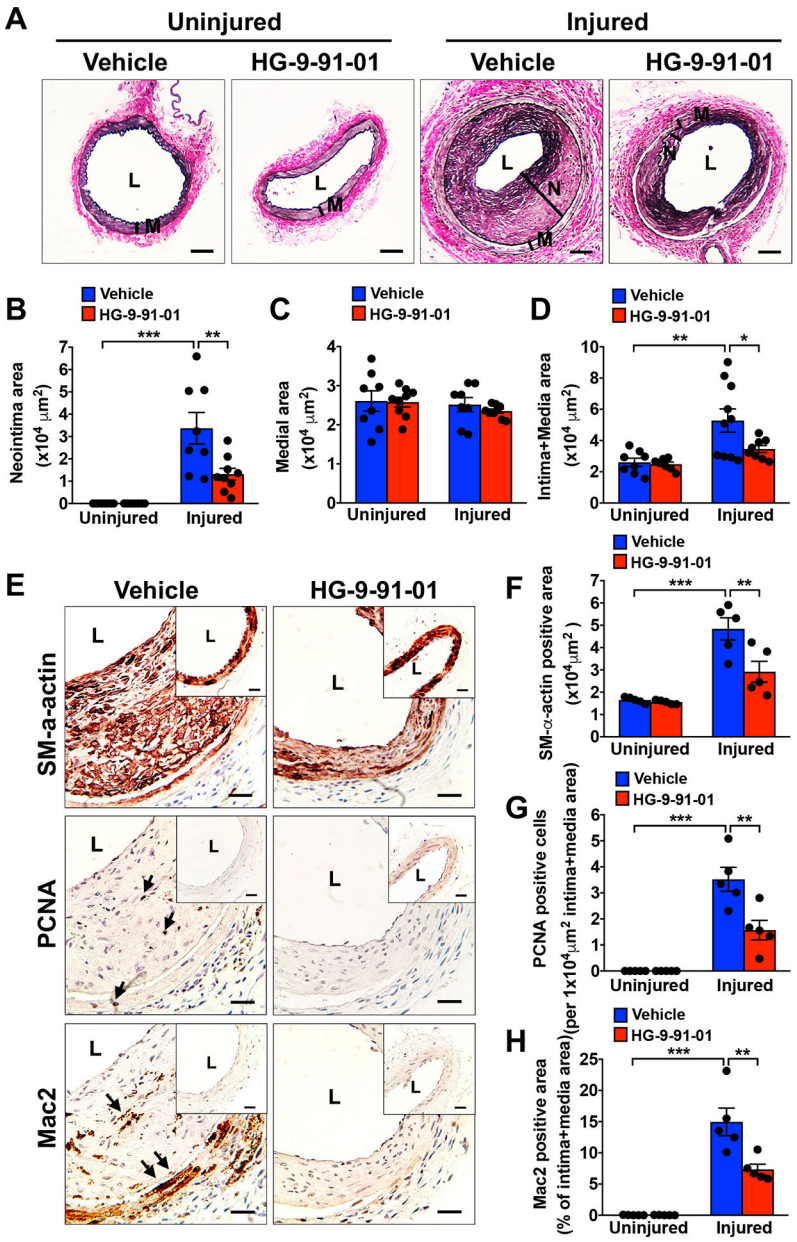

Figure 5. SIK inhibition reduces neointima formation following arterial injury.

The femoral artery wire injury procedure was used to induce neointima formation in mice. **A**. Representative VVG staining showing the effects of SIK inhibition on arterial injury-induced neointima formation. After wire injury on left femoral artery, a 50 μl of 20% pluronic F-127 gel containing 10 μM of SIK inhibitor HG-9–91–01 or vehicle was immediately applied around the injured vessel. Right femoral artery is uninjured vessel. Animals were harvested after 4 weeks. Elastic lamina was stained using VVG method. Scale bar, 50 μm. **B-D**. Morphometric analysis of intimal, medial and lumen areas by ImageJ software. n=8–9. **E**. Representative immunohistochemistry images showing the effects of SIK inhibition on SM-α-actin (SMC marker), PCNA (proliferation marker), and Mac2 (inflammation markers) after wire injury. Insets are uninjured vessels. Hematoxylin was

used for counterstaining. Scale bar, 25 μm. **F-H**. Quantitative results of the expression of SM-α-actin, PCNA, and Mac2. n=5. Data were analyzed by two-way ANOVA with multiple comparisons. ANOVA analysis was corrected with post hoc test. Values are mean ± SE. *$P < 0.05$, **$P < 0.01$, ***$P < 0.001$. N, neointima; M, media; L, lumen. Arrow, PCNA positive cells or Mac2 positive area.

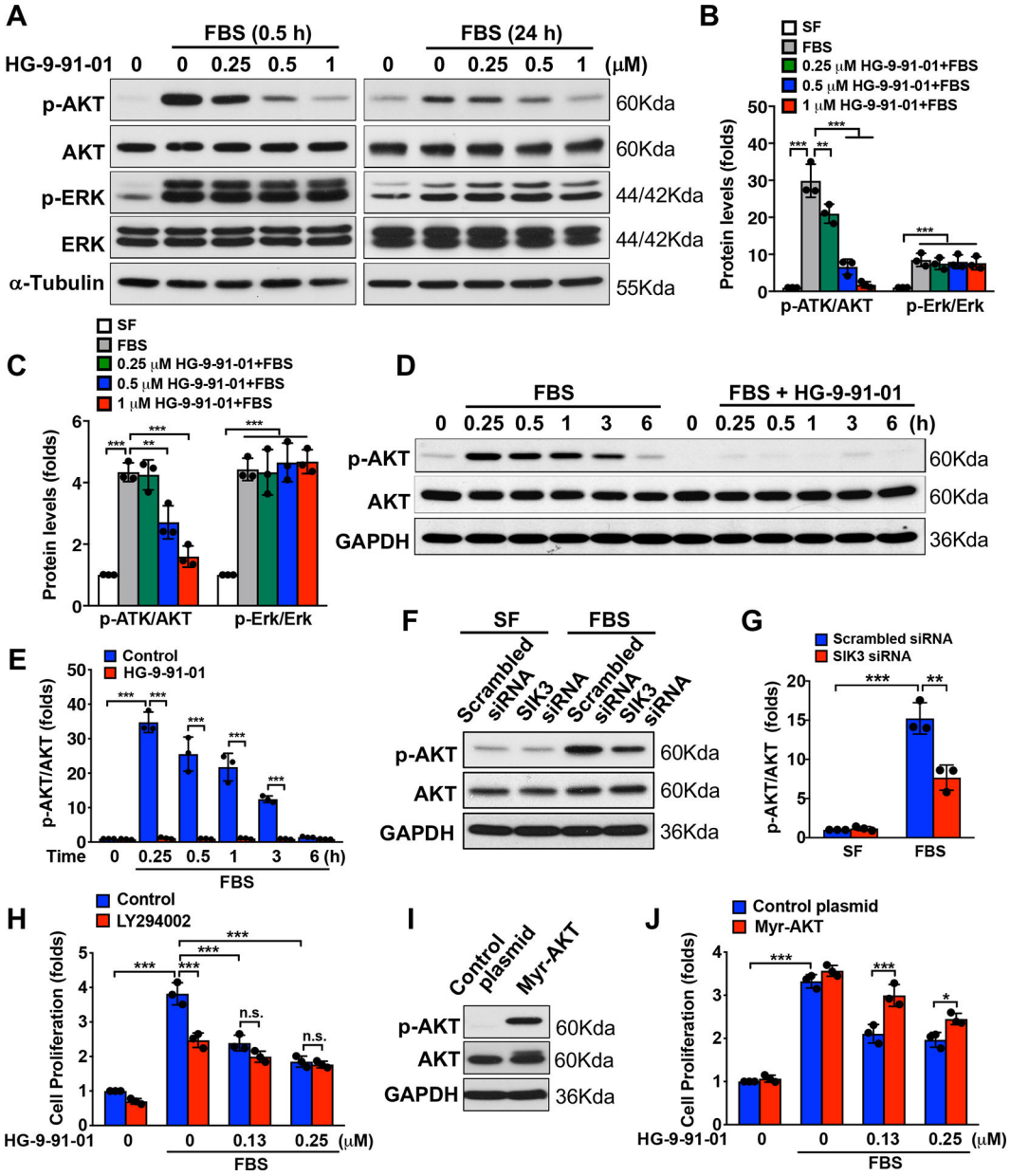

Figure 6. SIK inactivation suppresses SMC proliferation through inhibiting AKT signaling.

A. Representative western blotting images showing the effects of SIK inhibition on FBS-induced p-AKT and p-ERK1/2. Rat aortic SMCs were serum-free (SF) starved and then treated with the indicated concentrations of SIK inhibitor HG-9–91–01 for 0.5 h, followed by stimulated with 5% FBS for 0.5 h and 24 h. **B-C**. Quantitative results of p-AKT and p-ERK1/2. Data were normalized with total AKT or ERK1/2. **D–E**. Western blotting results showed that HG-9–91–01 time-dependently attenuated FBS-induced p-AKT. Rat aortic SMCs were serum-free starved and then treated with 1 μM of HG-9–91–01 for 0.5 h, followed by stimulation with 5% FBS for indicated time points. **F-G**. Knockdown of SIK3 decreased FBS-induced p-AKT. Rat aortic SMCs were transfected with 100 nM scrambled siRNA or SIK3 siRNA, then serum-free starved, followed by stimulation with

5% FBS for 24 h. **H**. Effects of a combination of SIK inhibitor and AKT inhibitor on SMC proliferation. Rat aortic SMCs were serum-free starved and then treated with 5 μM AKT inhibitor LY294002 and indicated concentrations of HG-9–91–01, followed by stimulation with 5% FBS for 48 h. **I-J**. Effects of a constitutively activated AKT on SIK inhibition-suppressed SMC proliferation. Rat aortic SMCs were transfected with Myr-AKT and control plasmids using electroporation, and then serum-free starved and treated with SIK inhibitor HG-9–91–01, followed by stimulation with 5% FBS for 48 h. **I**. Western blotting showed that transfection with Myr-AKT activated AKT signaling. **J**. Myr-AKT rescued SIK inhibition-suppressed SMC proliferation. Cell proliferation was assessed using SRB assay. Data were analyzed by two-way ANOVA with multiple comparisons. ANOVA analysis was corrected with post hoc test. Values are mean ± SD. n=3. $*P < 0.05$, $**P < 0.01$, $***P < 0.001$, n.s., no statistical significance.

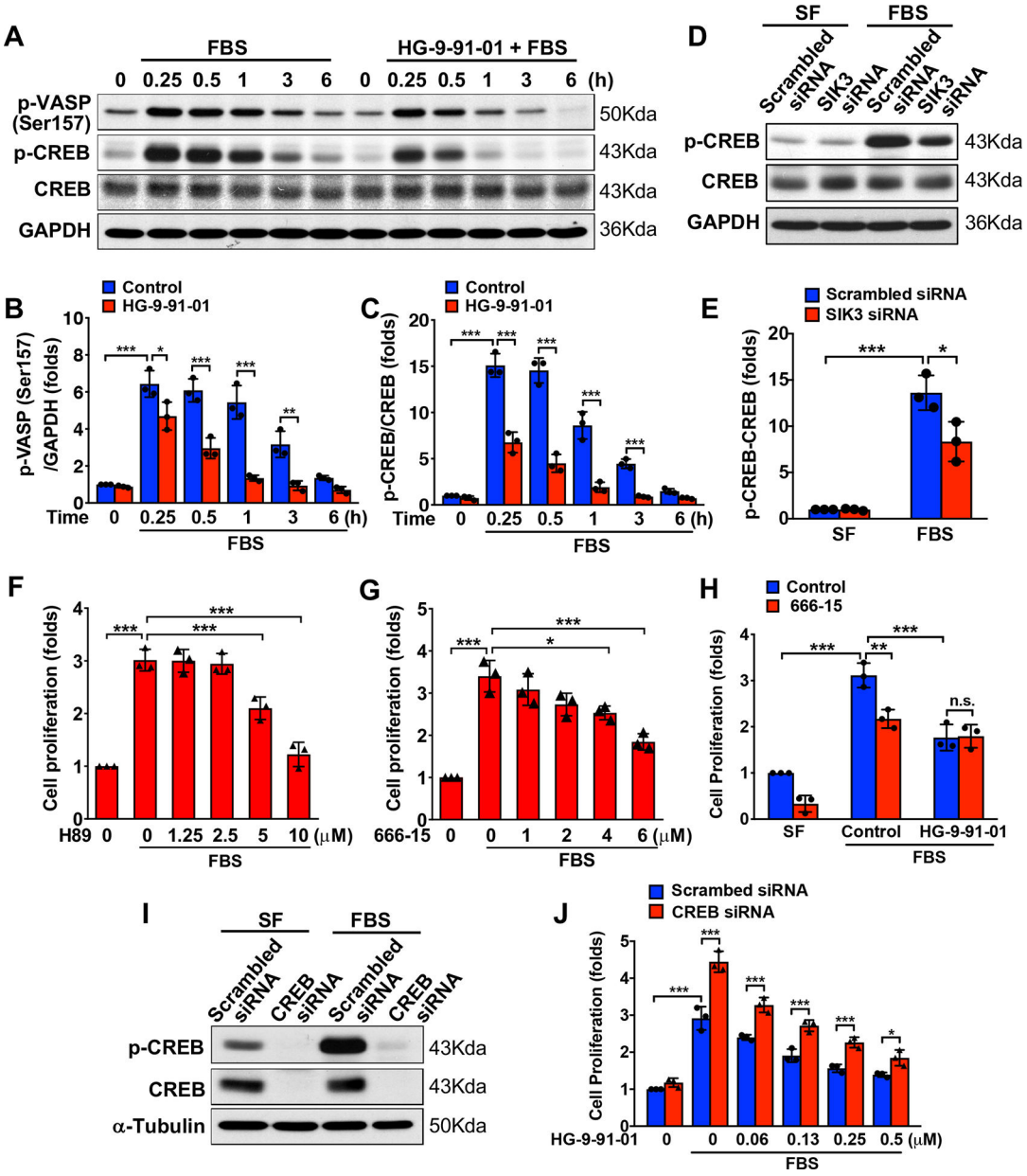

Figure 7. SIK inactivation suppresses SMC proliferation through down-regulating PKA-CREB signaling.

A. Representative western blotting images showing the effects of SIK inhibition on FBS-induced PKA-CREB signaling. Rat aortic SMCs were serum-free starved and then treated with 1 μM SIK inhibitor HG-9–91–01 for 0.5 h, followed by stimulation with 5% FBS for indicated time-points. PKA activity was assessed by its substrate p-Ser157-VASP. **B-C**. Quantitative results of p-Ser^{157}-VASP and p-CREB. Data were normalized with GAPDH or total CREB. **D–E**. Effects of SIK3 knockdown on FBS-induced PKA-CREB signaling. Rat aortic SMCs were transfected with 100 nM scrambled siRNA or SIK3 siRNA, then serum-free (SF) starved, followed by stimulation with 5% FBS for 24 h. **F-G**. Effects of inactivation of PKA or CREB on SMC proliferation. Rat aortic SMCs were serum-free starved and then treated with various concentrations of PKA inhibitor H89 or CREB

inhibitor 666–15 for 0.5 h, followed by stimulation with 5% FBS for 48 h. **H**. Effects of CREB signaling on SIK inhibition-suppressed SMC proliferation. Rat aortic SMCs were serum-free starved, then treated with 5 μM 666–15 in the presence of 0.25 μM HG-9–91–01, followed by stimulation with 5% FBS for 48 h. **I**. Western blotting showing knockdown efficiency of CREB siRNA. **J**. Effects of CREB knockdown on SIK inhibition-suppressed SMC proliferation. Rat aortic SMCs were transfected with 50 nM scrambled siRNA or CREB siRNA, then serum-free starved, followed by treatment with various concentrations of HG-9–91–01 for 48 h. Cell proliferation was assessed using SRB assay. Data were analyzed by one-way ANOVA or two-way ANOVA with multiple comparisons. ANOVA analysis was corrected with post hoc test. Values are mean ± SD. n=3. $*P < 0.05$, $**P < 0.01$, $***P < 0.001$, n.s., no statistical significance.

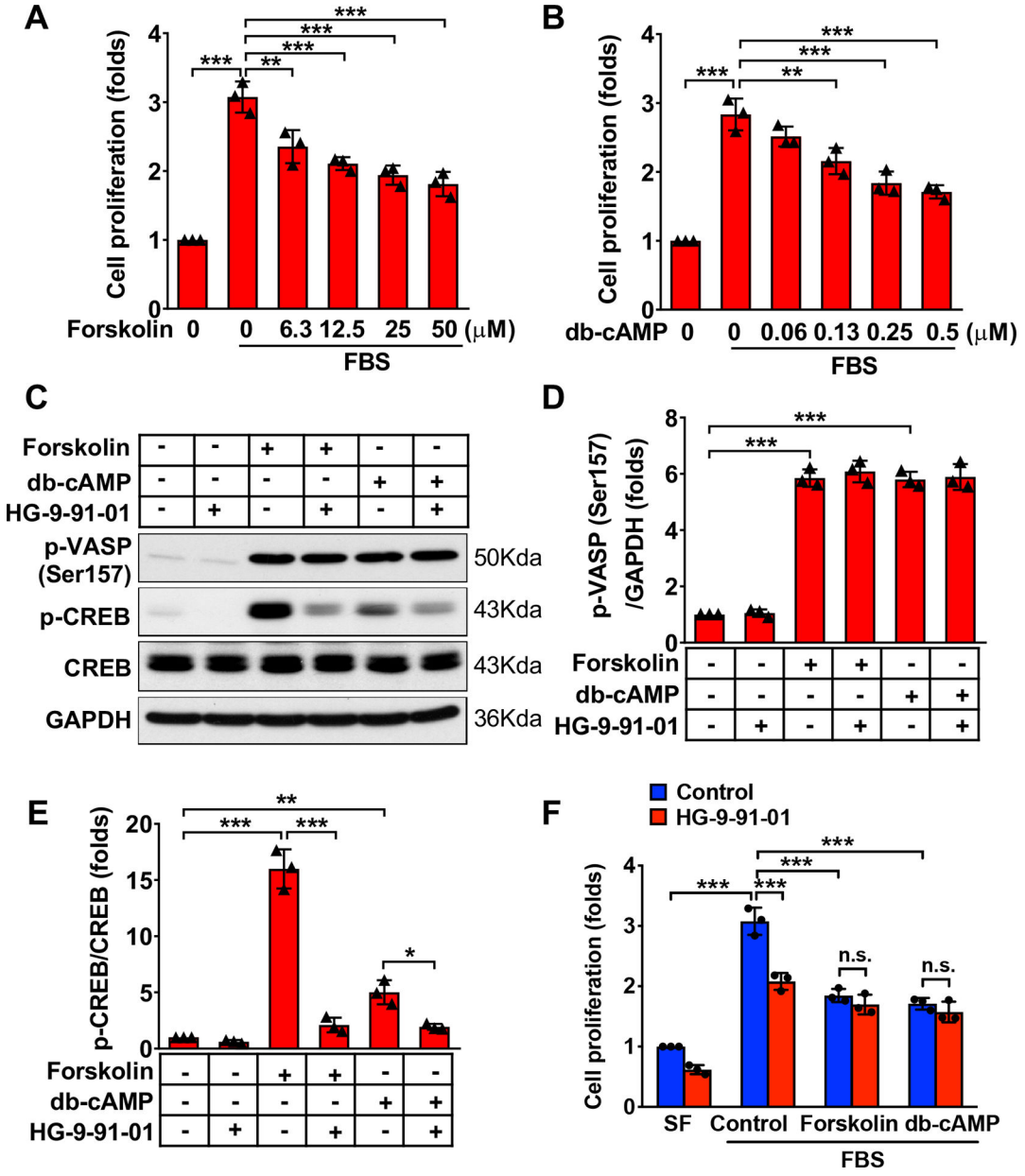

Figure 8. SIK inactivation suppresses cAMP-triggered CREB signaling.

A-B. Effects of elevated cAMP on SMC proliferation. Rat aortic SMCs were serum-free starved and then treated with various concentrations of Forskolin (an adenylyl cyclase activator) or db-cAMP (an cAMP analog), followed by stimulation with 5% FBS for 2 days. **C**. Representative western blotting images showing the effects of SIK inhibition on cAMP-mediated PKA/CREB signaling. Rat aortic SMCs were treated with 0.5 μM HG-9–91–01 for 0.5 h, and then treated with 100 μM forskolin or 0.5 mM db-cAMP for 0.5 h**. D**. Quantitative results of p-Ser^{157}-VASP expression. Data were normalized with GAPDH. **E**. Quantitative results of p-CREB. Data were normalized with total CREB. **F**. Effects of SIK inhibition on cAMP signaling-inhibited SMC proliferation. Rat aortic SMCs were treated with 0.5 μM HG-9–91–01 for 0.5 h and then treated with 100 μM forskolin or 0.5 mM

db-cAMP for 48 h. Cell proliferation was assessed using SRB assay. Data were analyzed by one-way ANOVA or two-way ANOVA with multiple comparisons. ANOVA analysis was corrected with post hoc test. Values are mean ± SD. n=3. $^{**}P < 0.01$, $^{***}P < 0.001$, n.s., no statistical significance.

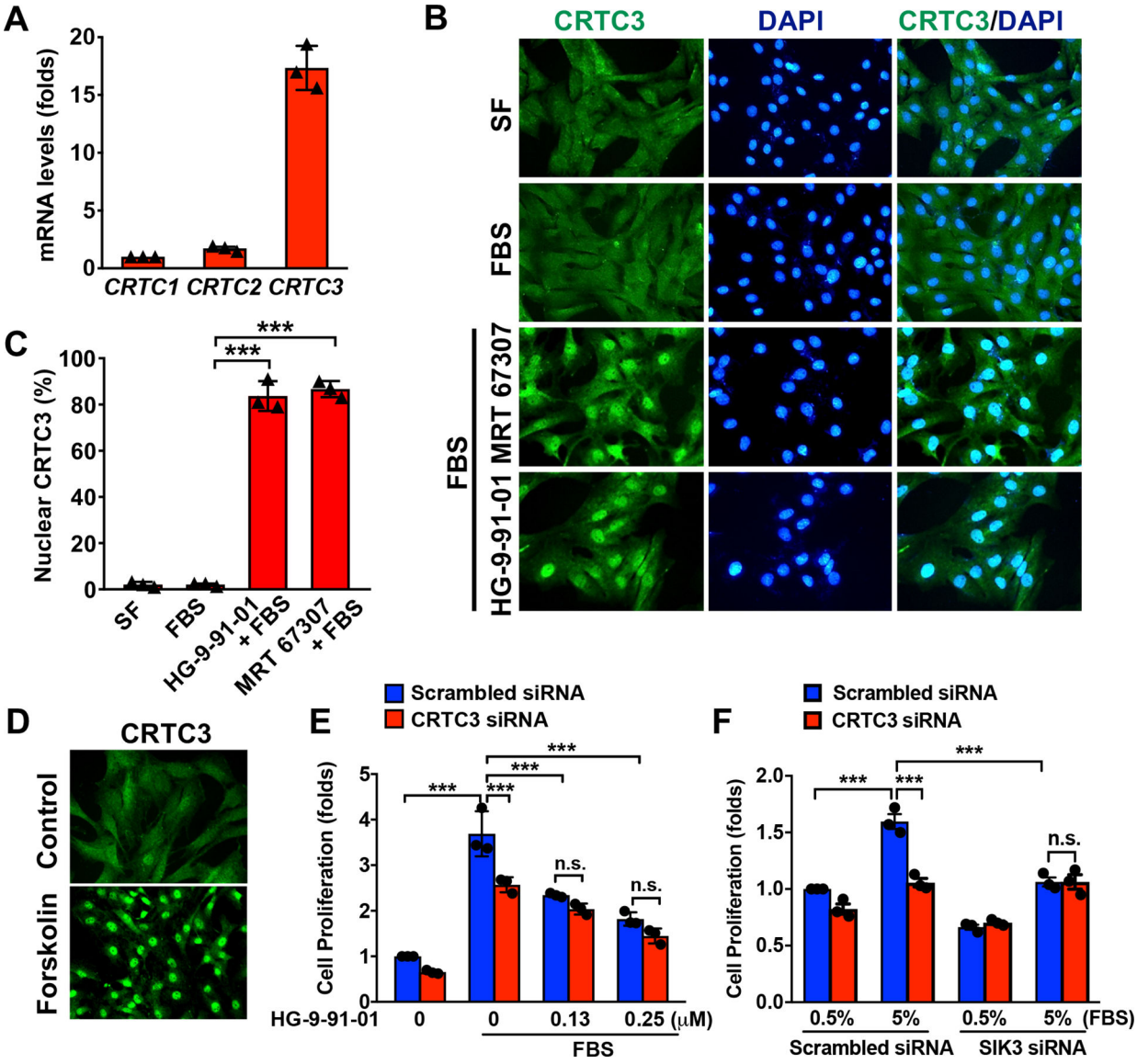

Figure 9. SIK inactivation-mediated CRTC3 signaling likely contributes to its anti-proliferative effect.

A. qPCR data showing the expression of CRTC1, 2, and 3 in cultured SMCs. **B**. Representative immunofluorescence images showing the effects of SIK inhibition on CRTC3 nuclear translocation. Rat aortic SMCs were serum-free (SF) starved and then treated with 1 μM HG-9–91–01 or 4 μM MRT67307 for 0.5 h, followed by stimulation with 5% FBS for 6 h. **C**. Quantitative results of nuclear CRTC3. **D**. Effects of forskolin-mediated cAMP signaling on CRTC3 nuclear translocation. Rat aortic SMCs were treated with 10 μM cAMP activator forskolin for 0.5 h. CRTC3 intracellular trafficking was determined by immunofluorescence staining using an anti-CRTC3 antibody. **E**. Effects of CRTC3 knockdown on SIK inactivation-suppressed SMC proliferation. Rat aortic SMCs were transfected with 100 nM scrambled siRNA or CRTC3 siRNA, serum-free starved, and then treated with HG-9–91–01 for 0.5 h, followed by stimulation with 5% FBS for 48 h. **F**. Effects of CRTC3 knockdown on SIK3 siRNA-suppressed SMC proliferation. Rat aortic

SMCs were transfected with 100 nM CRTC3 siRNA or SIK3 siRNA, or scrambled siRNA, 0.5% FBS starved, and then treated with HG-9–91–01 for 0.5 h, followed by stimulation with 5% FBS for 48 h. Cell proliferation was assessed using SRB assay. Data were analyzed by one-way ANOVA or two-way ANOVA with multiple comparisons. ANOVA analysis was corrected with post hoc test. Values are mean ± SD. n=3. ***$P < 0.001$, n.s., no statistical significance.

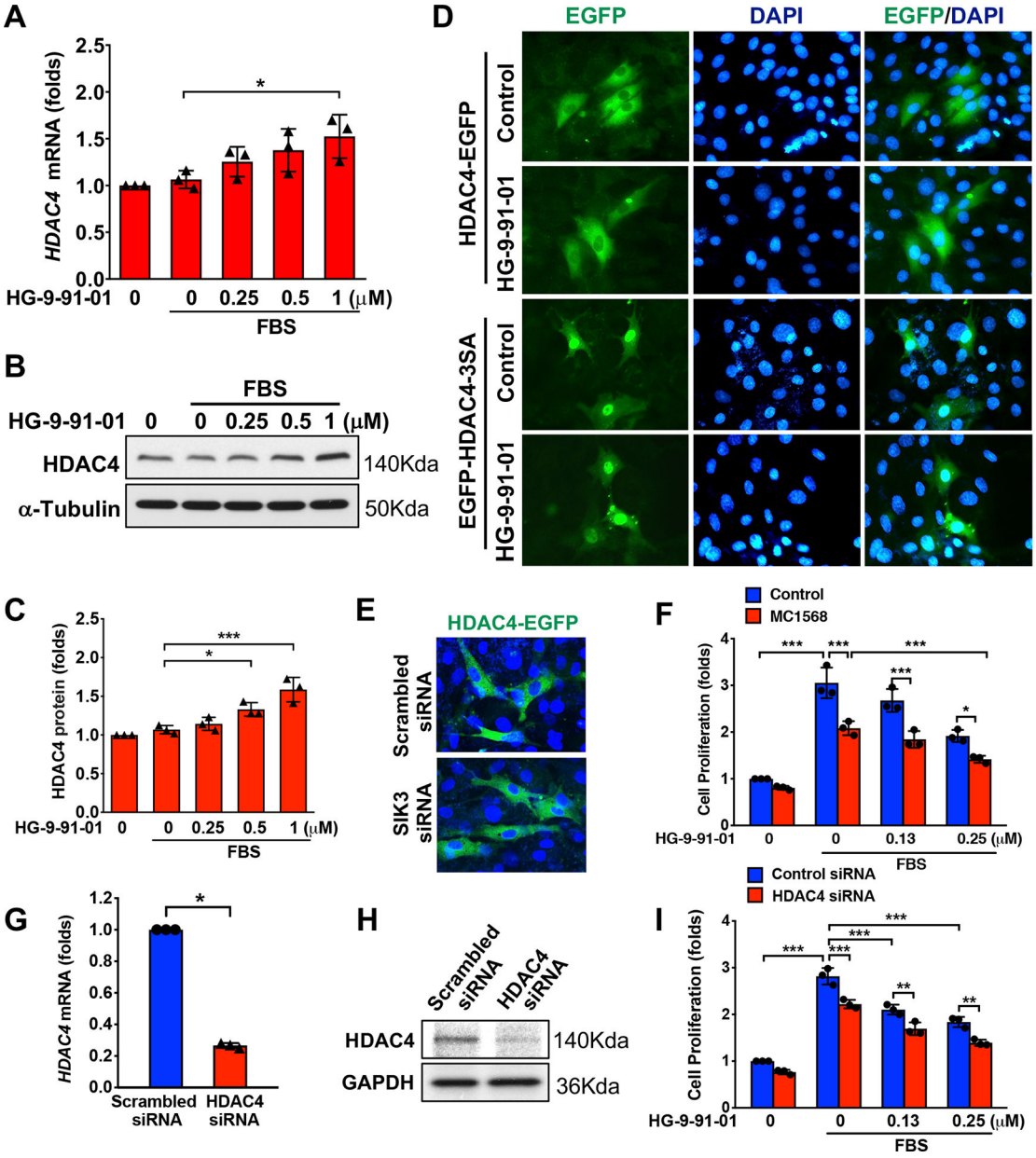

Figure 10. SIK inactivation-mediated suppression of SMC proliferation is independent of HDAC4.

A-C. Effects of SIK inhibition on mRNA and protein levels of HDAC4. Rat aortic SMCs were serum-free starved and then treated with various concentrations of HG-9–91–01 for 0.5 h, followed by stimulation with 5% FBS for 24 h. **D**. Representative immunofluorescence images showing the effects of SIK inhibition on HDAC4 intracellular trafficking. Rat aortic SMCs were transfected with pEGFP-HDAC4 or pEGFP-HDAC4–3SA using electroporation and then treated with 1 μM SIK inhibitor HG-9–91–01 for 24 h. Nuclei were stained with DAPI. **E**. Effects of SIK3 knockdown on HDAC4 nuclear translocation. Rat aortic SMCs were co-transfected with pEGFP-HDAC4 and SIK3 siRNA, or Scrambled siRNA using electroporation for 48 h, and then treated with 1 μM SIK inhibitor HG-9–91–01 for 6 h. **F**. Effects of HDAC4 inhibitor on SIK inhibition-suppressed SMC proliferation.

Rat aortic SMCs were serum-free starved, and then treated with 10 μM HDAC4 inhibitor MC1568, followed by stimulation with HG-9–91–01 for 0.5 h, followed by stimulation with 5% FBS for 48 h. **G-I**. Effects of HDAC4 knockdown on SIK inhibition-suppressed SMC proliferation. Rat aortic SMCs were transfected with 50 nM scrambled siRNA or HDAC4 siRNA, serum-free starved, and then treated with HG-9–91–01 for 0.5 h, followed by stimulation with 5% FBS for 48 h. qPCR and western blotting showing knockdown of HDAC4 (**G-H**). Cell proliferation was assessed using SRB assay. Data were analyzed by t test, one-way ANOVA or two-way ANOVA with multiple comparisons. ANOVA analysis was corrected with post hoc test. Values are mean ± SD. n=3. *$P < 0.05$, **$P < 0.01$, ***$P < 0.001$.